

GENETICS OF STRESS-INDUCED RESPONSES IN *DROSOPHILA*

APPROVED BY SUPERVISORY COMMITTEE

John M. Abrams, Ph.D.

Errol C. Friedberg, MD

Helmut Kramer, Ph.D.

Xiaodong Wang, Ph.D.

Dedicated to my parents,
Yahya and Fatma Akdemir

ACKNOWLEDGEMENTS

I would like to thank my advisor John M. Abrams for his patience, nourishing discussions, and guidance.

I would also like to thank my thesis committee, Errol Friedberg, Helmut Kramer, and Xiaodong Wang for their advice, which I would definitely use more.

Lastly, I would like to thank all past and present members of the Abrams' Lab for their help.

GENETICS OF STRESS-INDUCED RESPONSES IN *DROSOPHILA*

by

FATIH AKDEMIR

DISSERTATION

Presented to the Faculty of the Graduate School of Biomedical Sciences

The University of Texas Southwestern Medical Center at Dallas

In Partial Fulfillment of the Requirements

For the Degree of

DOCTOR OF PHILOSOPHY

The University of Texas Southwestern Medical Center at Dallas

Dallas, Texas

June 2006

Copyright

by

FATİH AKDEMİR, 2006

All Rights Reserved

GENETICS OF STRESS-INDUCED RESPONSES IN *DROSOPHILA*

FATIH AKDEMIR, Ph.D.

The University of Texas Southwestern Medical Center at Dallas, 2006

Mentor: JOHN M. ABRAMS, Ph.D.

Apoptosis is a highly conserved process responsible for elimination of cells during normal development and after cellular damage. Apical caspases that initiate caspase cascades are stimulated upon interaction with adaptor molecules. The *Drosophila* adaptor protein Dark, a homolog of nematode Ced-4 and mammalian Apaf-1, regulates the apical caspase Dronc, through interactions involving respective caspase recruitment domains (CARD). Dronc is the only caspase in the fly genome with a caspase recruitment domain. Here I pursue functional characterization of

dronc and *dark* animals especially to find out whether they are required for all programmed cell death and whether they have distinct functions. *dronc* mutants have extensive hyperplasia of hematopoietic tissues and adult structures lacking *dronc* are disrupted for fine patterning. In diverse models of metabolic injury, *dronc*⁻ cells are completely insensitive to induction of cell killing. I also show the generation and functional characterization of *dark* null mutant animals. Using *in vivo* and *ex vivo* assays, I demonstrate a global apoptogenic requirement for *dark* and show that a required focus of *dark*⁻ organismal lethality maps to the central nervous system. Finally I show functional similarities of *dronc* and *dark* null mutants by a diverse set of experiments. Together these findings illustrate broad requirements for Dark and Dronc in adaptive responses during stress-induced apoptosis and in normal cell death.

Treatment of cells with DNA-damaging agents upregulates the transcription of many genes, many of which are not functionally characterized. In a series of independent studies I characterize an ionizing radiation (IR)-induced gene, CG17836, designated as *xrp1*. *Xrp1* is robustly responsive to IR, and it is a nuclear protein with DNA-binding activity as inferred from domain structure. I have characterized two different loss-of-function mutants of *xrp1*. In a loss-of-heterozygosity (LOH) assay *xrp1* mutant animals display higher genomic instability than

wild types after IR challenge. Even though *xrp1* is not required for apoptosis or cell cycle arrest after IR treatment in animals, surprisingly, its overexpression in cell culture prevents cell proliferation. Thus, Xrp1 might maintain genomic stability by modulating cell cycle checkpoints upon IR exposure.

TABLE OF CONTENTS

Title	
Dedication	
Acknowledgements	
Title Page	
Abstract.....	v
Table Of Contents.....	viii
Prior Publications.....	xi
List Of Figures.....	xii
List Of Tables.....	xiv
List Of Abbreviations.....	xv
 Chapter One: Introduction.....	 1
Apoptosis	1
Apoptosis In <i>Drosophila</i>	4
Legends and Figures.....	6
 Chapter Two: The Apical Caspase, <i>Dronc</i> , Governs	
Unprogrammed Cell Death In <i>Drosophila</i>	7
Abstract.....	7
Introduction.....	8
Materials And Methods.....	10
Results.....	13
<i>Dronc</i> Is Required For Stress-Induced Apoptosis.....	13
<i>Dronc</i> Is Required For Fine Patterning Of	
The Adult Eye.....	16
The Dronc/Dark Axis Is Required For Proper	

Maintenance Of Adult Wing Tissue.....	17
Defect In Exit From Cell Cycle Arrest In <i>Dronc</i> Mutants After Ionizing Radiation (IR).....	18
Discussion.....	20
Legends and Figures.....	23
Chapter Three: Generation And Functional Characterization Of	
<i>Dark</i> Null Mutant Animals.....	32
Abstract.....	32
Introduction.....	33
Materials And Methods.....	35
Results.....	38
<i>Dark</i> ⁸² Is Null Allele.....	38
Elimination Of Maternal And Zygotic <i>Dark</i>	38
Tissue-Specific Restoration In The CNS Reverses <i>Dark</i> ⁻ Lethality.....	40
A Caspase Cleavage Site In <i>Dark</i> Confers Hypermorphic Gene Activity When Mutated.....	41
Functional Similarities Of <i>Dronc</i> And <i>Dark</i> Null Mutations.....	42
Discussion.	44
Future Directions.....	47
Legends and Figures.....	50
Chapter Four: A Novel Radiation Responsive Gene, <i>Xrp1</i> , Inhibits Cell Proliferation And Maintains Genomic	
Stability After Exposure To Genotoxic Stress.....	60
Abstract.....	60

Introduction.....	61
Materials And Methods.....	65
Results.....	70
Ionizing Radiation Induces Xrp1 Transcription.....	70
Identification And Molecular Characterization Of Xrp1 Mutant Strains.....	71
J3E1 Allele.....	72
Synthetic Allele.....	73
Xrp1 Promotes Genomic Stability After Genotoxic Stress.....	74
Xrp1 Overexpression Prevents Cell Proliferation.....	76
Discussion.....	79
Future Directions.....	84
Legends and Figures.....	86
 Bibliography.....	 99
Vitae	

PRIOR PUBLICATIONS

Akdemir F, Christich A, Sogame N, Abrams JM. A novel radiation responsive gene, *xrp1*, inhibits cell proliferation and maintains genomic stability after exposure to genotoxic stress. In preparation.

Akdemir F, Farkas R, Chen P, Juhasz G, Medved'ova L, Sass M, Wang L, Wang X, Chittaranjan S, Gorski SM, Rodriguez A, Abrams JM. Autophagy occurs upstream or parallel to the apoptosome during histolytic cell death. *Development* 133(8), 1457-65, 2006

Chew SK*, Akdemir F*, Chen P*, Lu WJ, Mills K, Daish T, Kumar S, Rodriguez A, Abrams JM. The apical caspase *dronc* governs programmed and unprogrammed cell death in *Drosophila*. *Dev Cell* 7(6), 897-907, 2004

* equal contribution

LIST OF FIGURES

FIGURE 1.1. A SIMPLIFIED MODEL OF <i>DROSOPHILA</i> APOPTOTIC MACHINERY.....	6
FIGURE 2.1. <i>DRONC</i> IS REQUIRED FOR STRESS-INDUCED APOPTOSIS.....	23
FIGURE 2.2. STRESS RESISTANCE OF <i>DRONC</i> MUTANT HEMOCYTES CONFIRMED BY FLOW CYTOMETRY...	24
FIGURE 2.3. <i>DRONC</i> IS REQUIRED FOR EFFECTOR CASPASE ACTIVITY.....	26
FIGURE 2.4. HYPERPLASIA OF BLOOD CELLS IN <i>DRONC</i> MUTANT ANIMALS.....	27
FIGURE 2.5. <i>DRONC</i> IS REQUIRED FOR FINE PATTERNING OF THE RETINA.....	28
FIGURE 2.6. WINGS MOSAIC FOR <i>DRONC</i> DISPLAY BLACK BLEMISHES.....	29
FIGURE 2.7. DELAYED EXIT FROM CELL CYCLE ARREST IN <i>DRONC</i> MUTANTS AFTER IONIZING RADIATION (IR).	30
FIGURE 3.1. GENERATION OF <i>DARK</i> ⁸² NULL MUTATION.....	50
FIGURE 3.2. <i>DARK</i> IS ESSENTIAL FOR EMBRYONIC PROGRAMMED CELL DEATH (PCD).....	51
FIGURE 3.3. <i>DARK</i> IS REQUIRED FOR UNPROGRAMMED APOPTOSIS.....	52
FIGURE 3.4. NORMAL GROSS MORPHOLOGY OF GERMLINE OF THE CNS-RESCUED <i>DARK</i> ⁸²	55

FIGURE 3.5. ALTERATION OF A CASPASE CLEAVAGE SITE PRODUCES A HYPERMORPHIC DARK VARIANT.....	56
FIGURE 3.6. <i>DARK</i> OR <i>DRONC</i> MUTANTS DISPLAY RESISTANCE TO IONIZING RADIATION (IR)-INDUCED APOPTOSIS.	57
FIGURE 3.7. SIMILAR TO <i>DRONC</i> , WINGS MOSAIC FOR <i>DARK</i> DISPLAY BLACK BLEMISHES.....	58
FIGURE 3.8. CONTRARY TO <i>DRONC</i> MUTANTS, ABSENCE OF HYPERPLASIA OF BLOOD CELLS IN <i>DARK</i> MUTANT ANIMALS.....	59
FIGURE 4.1. STRESS INDUCTION OF XRP1 OCCURS BY TRANSCRIPTION.....	86
FIGURE 4.2. IDENTIFICATION AND MOLECULAR CHARACTERIZATION OF THE XRP1 LOCUS.....	89
FIGURE 4.3. XRP1 SYNTHETIC MUTATION.....	90
FIGURE 4.4. XRP1 PROMOTES GENOMIC STABILITY AFTER GENOTOXIC STRESS.....	92
FIGURE 4.5. <i>XRP1</i> (J3E1 STRAIN) IS NOT REQUIRED FOR IONIZING RADIATION (IR)-INDUCED APOPTOSIS....	93
FIGURE 4.6. CELL CYCLE ARREST AFTER IONIZING IS UNAFFECTED BY LOSS OF XRP1.....	94
FIGURE 4.7. XRP1 OVEREXPRESSION PREVENTS CELL PROLIFERATION.....	95
FIGURE 4.8. ANALYSIS OF XRP1-MEDIATED PROLIFERATION ARREST BY FLOW CYTOMETRY.....	97

LIST OF TABLES

TABLE 2.1. <i>DRONC</i> IS REQUIRED FOR APOPTOSIS INDUCED BY BROAD RANGE OF STRESS STIMULI.....	25
TABLE 3.1. CNS-SPECIFIC RESCUE OF <i>DARK</i> ⁸² LETHALITY BY THE EXPRESSION OF WILD- TYPE <i>DARK</i> ALLELE.....	54

LIST OF DEFINITIONS

ATM – Ataxia telangiectasia mutated

ATR – Ataxia telangiectasia and Rad3 related

CARD – Caspase Activation-Recruitment Domain

Caspase – CysteinyI aspartate-specific protease

Ced – Cell death defective

Dark – Drosophila apaf-1 related killer

Dcp1 – Drosophila caspase 1

Debcl – Drosophila executioner bcl

DED – Death Effector Domain

Dmp53 – Drosophila melanogaster p53

Drice – Drosophila ICE homolog

Dronc – Drosophila nedd2-like caspase

GFP – Green fluorescence protein

Hid – Head involution defective

IAP – Inhibitor of apoptosis protein

IR– Ionizing radiation

LOH – Loss of heterozygosity

Mwh – Multiple wing hair

PCD – Programmed Cell Death

RIPD – Radiation induced p53 dependent

Rpr – Reaper

Skl – Sickle

Xrp1 – X-ray responsive protein 1

WT – wild-type

CHAPTER ONE¹

INTRODUCTION

Apoptosis

Apoptosis, a form of programmed cell death, has distinct characteristics from necrosis. Kerr and colleagues (Kerr et al., 1972) first made a clear distinction between cell deaths during animal development (apoptosis) and pathological cell deaths during ischemia (necrosis). During necrosis cells and organelles usually swell and rupture, leaking their contents, which induces tissue inflammatory responses (probably through HMGB1 (Scaffidi et al., 2002)). In contrast, during apoptosis cells shrink and they are phagocytosed without stimulating inflammation. Because of common characteristics of apoptotic cell deaths in different systems, Kerr and colleagues thought there is an intracellular death program responsive to different stimuli (Kerr et al., 1972).

Cell lineage studies of *C. elegans* by Horvitz and colleagues have demonstrated a genetic program for apoptotic cell death (Ellis and Horvitz, 1986). They found that 131 cells that normally die during development

¹Portions of Chapters 1, 2 and 3 are excerpted from my two publications.

persist in *ced-3* or *ced-4* mutants (Ellis and Horvitz, 1986). In contrast, *ced-9* loss-of-function activated the cell death program in most cells, if not all. Another line of studies by Korsmeyer and colleagues has identified a protein overexpressed in B-cell lymphomas due to translocation, Bcl-2 (Vaux et al., 1988). Prevention of cell death in *C.elegans* by Bcl-2 overexpression (Vaux et al., 1992) demonstrated the conservation of the death program in the worm and mammals.

Cloning of the *ced-3* gene (Yuan et al., 1993) was a cornerstone to understand molecular mechanism of apoptosis. It turned out that the *ced-3* gene encodes a protein similar to a cysteine protease, interleukin-1 β converting enzyme (ICE, now Caspase-1). We now know that caspases, including *ced-3*, are cysteine proteases and they form the core machinery of the apoptotic program (Yuan and Horvitz, 2004).

Biochemical studies of Wang and colleagues established the role of mitochondria in apoptosis, and formation and function of a complex called the apoptosome. Upon a death stimulus, cytochrome c is released from mitochondria and binds to Apaf-1 (*ced-4* homolog). Cytochrome c and dATP-bound Apaf-1 interacts with and activates Caspase-9 through CARD domains. Activated Caspase-9 then cleaves and activates an effector caspase, Caspase-3 (Li et al., 1997; Liu et al., 1996; Zou et al., 1997). By cleaving other protein substrates, caspase-3 and other effector

caspases execute the apoptotic death program resulting in elimination of the cell. In addition to this so-called intrinsic pathway, mediated by the apoptosome, there is an extrinsic pathway regulated by cell surface receptors. Ligand binding to death receptors (e.g. Fas) triggers oligomerization of the receptor. The adaptor protein FADD interacts with the receptor and recruits caspase-8, forming a complex called the DISC. Activated caspase-8 then cleaves caspase-3, similar to caspase-9 (Danial and Korsmeyer, 2004).

Caspases are the effectors of the death program and based on the length of their prodomains they can be classified into two groups: apical (or initiator) and effector caspases. Adaptor proteins such as Apaf-1 and FADD interact with, and activate, apical caspases, caspase-9 and caspase-8 respectively. Activated apical caspases in turn cleave effector caspases such as caspase-3. Apoptotic pathways are subject to regulation by multiple ways. For instance Bcl-2 family proteins are the major regulators of the cytochrome c release (Gross et al., 1999). Inhibitor of apoptosis proteins (IAPs) can bind to activated caspases and prevent their activity (Deveraux et al., 1997). IAPs themselves can be regulated by other factors such as Smac (Du et al., 2000).

Apoptosis in *Drosophila*

The fly genome encodes seven caspases family (Kumar and Doumanis, 2000). Caspases are cysteinyl aspartate-specific proteinases and synthesized as dormant proenzymes. Upon death stimuli these proenzymes are cleaved and activated (Danial and Korsmeyer, 2004; Salvesen and Duckett, 2002; Shi, 2002). Regarding to prodomain structure, Dredd (Chen et al., 1998) and Dronc (Dorstyn et al., 1999), are like apical or initiator caspases; Dredd has death effector-like domains (DEDs) and Dronc contains a caspase recruitment domain (CARD) through which they interact with adaptor proteins. The other long prodomain caspase is Strica and it has unusual serine/threonine-rich prodomain. The other four caspases Drice, DCP1, Decay, Damm resemble effector or executioner caspases, based on their short prodomains.

Apical and effector caspases lie at the core of the apoptotic program (Danial and Korsmeyer, 2004). Upon interaction with adaptor molecules, apical caspases are stimulated to activate effector caspases by proteolysis. Dark, the *Drosophila* homolog of nematode Ced-4 and mammalian Apaf-1, is thought to regulate the apical caspase Dronc, through interactions involving respective caspase recruitment domains (CARD) (reviewed in (Mills et al., 2005)). As in mammalian systems, fly

caspases are also subject to negative regulation by IAP proteins (Danial and Korsmeyer, 2004) and, among *Drosophila* members of this family, DIAP1 is known to exert important control over apoptosis (Goyal, 2001; Wang et al., 1999) (Figure 1.1). This protein binds Dronc and the effector caspase Drice, inhibiting the activity of each via multiple mechanisms (Ditzel et al., 2003; Hays et al., 2002; Martin, 2002; Meier et al., 2000b; Ryoo et al., 2002; Wilson et al., 2002; Wing et al., 2002b). DIAP1 itself is under tight regulation and effectively antagonized by proapoptotic proteins (*reaper (rpr)*, *grim*, *hid* and *skl*) encoded in the *Reaper* region (Chai et al., 2003; Christich et al., 2002; Silke et al., 2003; Wing et al., 2002a; Wing et al., 2002b; Wing et al., 2001; Wu et al., 2001; Yoo et al., 2002; Zachariou et al., 2003). Together, these linked genes specify virtually all programmed cell death (PCD) in the fly embryo, since the combined deletion of these eliminates PCD at this stage (Abrams, 1999).

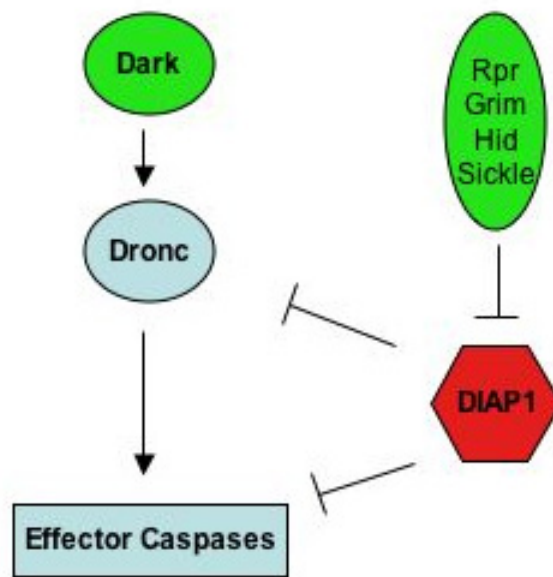


Figure 1.1. A simplified model of *Drosophila* apoptotic machinery

CHAPTER TWO

THE APICAL CASPASE, *DRONC*, GOVERNS UNPROGRAMMED CELL DEATH IN *DROSOPHILA*

Abstract

Dronc is the only caspase in the fly genome with a caspase recruitment domain. Here I present functional characterization of *dronc* null-mutant animals, using an allele generated by others in the lab. *dronc* mutants have extensive hyperplasia of hematopoietic tissues. Adult structures lacking *dronc* are disrupted for fine patterning. In diverse models of metabolic injury, *dronc*⁻ cells are completely insensitive to induction of cell killing. These findings illustrate broad requirements for this apical caspase in adaptive responses during stress-induced apoptosis.

Introduction

Studies that examine the functional properties of *Drosophila* caspases have primarily relied upon on multigenic deficiencies, dominant negative variants (Meier et al., 2000a) or injected dsRNAs (Quinn et al., 2000). Genetic studies have established requirements for *dredd* in innate immunity (Leulier et al., 2000) and a role for *dcp1* in stress-induced death in the ovary (Laundrie et al., 2003). As the only CARD-domain containing caspase encoded in the fly genome, *dronc* is thought to be crucial for programmed cell death (PCD) (Dorstyn et al., 1999; Meier et al., 2000a). Support for this inference includes detection of Dronc/Dark complexes (Dorstyn et al., 2002; Quinn et al., 2000) RNAi studies (Quinn et al., 2000) and dominant negative transgenes which, in recent studies, have also implicated *dronc* in functions unrelated to PCD (Huh et al., 2004b). At the time of this work, mutations in *dronc* had not been isolated and, hence, the actual requirements for this apical caspase in development and in PCD were not known. To examine these issues, genetic analyses of this locus was conducted in the lab by others and established that *dronc* is a recessive, lethal gene. Animals lacking a zygotic source of *dronc* arrested as early pupae, were defective for PCD in some tissues and showed a genetic interaction with *dark*. These mutants exhibit a range of defects,

including severe hyperplasia of blood cells, supernumerary neuronal cells and head involution failure.

Here I use clonal analyses to test requirements for *dronc* later in development. I found that adult tissues were affected, since fine patterning of the eye was disrupted and a progressive, age-dependent degeneration of wing tissue occurred. Cell proliferation dynamics was modified in *dronc* mutant larval wing discs after ionizing radiation treatment. Furthermore, in diverse models of metabolic injury, *dronc*⁻ cells were completely insensitive to induction of cell killing. These studies establish *dronc* as an essential regulator of cell number in development and reveal broad requirements for this apical caspase in adaptive responses during stress-induced apoptosis.

Materials and methods

Fly strains. Hml-UAS:GAL4-GFP was obtained from Bloomington Stock Center. *dronc*⁵¹ is a null mutation generated in the lab by other lab members and *dronc*^{51^{drf}} strain has a *dronc* rescue transgene in *dronc*⁵¹ background (Chew et al., 2004). In order to make conditional mutants of *dronc*, FRT79 is recombined with *dronc*⁵¹. The method for producing wing clones was as in (Vegh and Basler, 2003). FRT-*dronc*⁵¹ refers to *Vg-GAL4:UAS-FLP* / +; *FRT79/dronc*⁵¹*FRT79*, and FRT refers to *Vg-GAL4:UAS-FLP* / +; *FRT79/FRT79*. The method for producing eye clones was adopted from (Stowers and Schwarz, 1999). In this case, FRT-*dronc*⁵¹ refers to *ey-GAL4:UAS-FLP*/+; *GMR-hid* *l(3)CL-L[1] FRT79/dronc*⁵¹*FRT79*, and FRT refers to *ey-GAL4:UAS-FLP*/+; *GMR-hid* *l(3)CL-L[1] FRT79/FRT79*.

Ex vivo Hemocyte Analyses. L3 instar larvae were washed thoroughly for 3 min in the following solutions - water, 70% ethanol, water, 50% bleach, water, 70% ethanol and water again. Wild type and mutant larvae were submerged and dissected in PBS. The liquid containing hemolymph was filtered with synthetic mesh (35XX Nitex), washed 3 times with PBS, each time pelleting for 5 minutes at 1500 rpm. The aspirates were washed one final time with Schneider's media (GIBCO) supplemented with 10% FCS and 50 µg/ml gentamycin. The hemocytes were plated at densities of

~80,000-100,000 per well in 96-well plates with fresh media. For stress treatments, hemocyte aspirates were treated separately 1 hour after plating with the following agents at the concentrations noted: CHX (100 μ M), actinomycin D (10 μ M), etoposide (1 mM), ethanol (1%), DMSO (1%), small molecule Smac mimetic (10 μ M) (Li et al., 2004). Blebbing was used to quantify cell death and surviving cell counts were normalized to an untreated plate. Flow cytometry was conducted ~8 hr post treatment on a FACScan machine using Cell Quest software.

Microscopy and imaging. For imaging following systems were used: Axioplan 2 microscope (Zeiss) with an Hamamatsu monochrome digital camera, Axiovert 100 M (Zeiss) and Eclipse TE300 (Nikon) inverted microscopes with Axiocam MRC color digital camera (Zeiss), and Stemi SV6 dissecting microscope (Zeiss) with a Canon digital camera. Scanning electron microscopy was done as in (Chen et al., 1996), except that the samples were not fixed.

Immunohistochemistry. It has been performed as in Chapter-4 except that fluorescein-labelled anti-rabbit secondary antibody (Vector Laboratories) was used for detection.

Caspase Assays. For hemocyte lysates, cells were prepared as described in the “*Ex Vivo* Hemocyte Analysis” section. Hemocytes were treated with CHX for 8 hr, then lysed in Buffer A (20 mM HEPES–KOH

pH 7.5, 10 mM KCl, 1.5 mM MgCl₂, 1 mM sodium EDTA, 1 mM sodium EGTA, 1 mM dithiothreitol and 0.1 mM phenylmethylsulfonyl fluoride) supplemented with 0.5% Triton-X 100. 10µg of protein extract was incubated with 10 µM Ac-DEVD-AFC or Ac-TQTD-AFC (Calbiochem) substrate in a final volume of 100 µl in a 96 microtiter plate. Fluorescence was monitored over time with excitation at 400 nm and emission at 505 nm in a SpectraFluor Plus plate reader.

Results

***dronc* is required for stress-induced apoptosis**

To examine the function of *dronc* in unprogrammed cell death, we measured responses in *ex vivo* cultures of larval hemocytes treated with pro-apoptotic agents (see methods). To facilitate the analysis, hemocytes were labeled with green fluorescent protein (GFP) using the *Hml-GAL4:UAS-GFP* marker chromosome. In stark contrast to wild type hemocytes, which were acutely reactive to these stressors, *dronc*⁵¹ hemocytes were remarkably insensitive. For example, cycloheximide (CHX) triggers widespread apoptosis in hemocytes from wild type animals within 8 hrs (Figure 2.1A,B) yet no apoptosis is detected in hemocytes from *dronc*⁵¹ animals (Figure 2.1C,D), even when 10 fold higher concentrations of cycloheximide were applied (not shown). This effect was not simply a delay in the kinetics of apoptosis since *dronc*⁵¹ cells were equally unresponsive at 20hrs and, even after 48hrs in cycloheximide, *dronc*⁵¹ cells were evidently alive and continued to exhibit changes in shape. Stress resistance of *dronc* mutant hemocytes was also confirmed by flow cytometry (Figure 2.2). Hemocyte aspirates expressing *Hml-GAL4:UAS-GFP* from wild type and *dronc*⁵¹ larvae were treated with CHX and flow cytometric analysis was performed 8 hrs later. Flow cytometric

analysis detects CHX induced apoptosis as loss of GFP expressing cells. Viable, GFP positive cells are lost in CHX-treated wild type but not *dronc*⁵¹ cultures (Figure 2.2).

The resistance to pro-apoptotic agents was not confined to protein synthesis inhibitors. For example, marked insensitivity was also documented in *dronc*⁵¹ hemocytes after exposure to Actinomycin D (transcription inhibitor), etoposide (Topoisomerase II inhibitor), ethanol and a small molecule Smac mimetic (Li et al., 2004) (Table 2.1). In the course of these studies, we also noticed that constitutive apoptosis in these primary cultures was influenced by the absence of *dronc*. For instance, at any given time, 2-3 % of hemocytes from wild type animals were typically apoptotic. In contrast, apoptotic hemocytes from *dronc*⁵¹ animals were exceptionally rare in these *ex vivo* preparations (note that statistical indicators of % death in *dronc*⁵¹ samples arise predominantly, if not exclusively, from variance in plating efficiencies) (Table 2.1). Together, these results establish a pivotal role for *dronc* as a mediator of stress-induced apoptosis.

To substantiate these findings, we extended these studies using an enzymatic assay to detect effector caspase activity (Figure 2.3). DEVD is a peptide substrate for effector caspases and DEVDase activity of hemocyte lysates derived from larvae of indicated genotypes (treated with

or without CHX) was measured. When stimulated with CHX, hemocytes from wild type or *dronc*^{51:drf} rescued animals show pronounced induction of DEVDase activity. In stark contrast, hemocytes derived from *dronc*⁵¹ animals were completely devoid of DEVDase (Figure 2.3) and, in a similar assay they were also negative when measured for PARP cleavage activity (Chew et al., 2004). While these data directly establish a fundamental role for Dronc in the context of stress-induced effector caspase activation, they also highlight two additional findings worth noting here. First, using this measure of genetic activity, *drf* (*dronc* rescue fragment) transgene restores some, but not all, of wild type *dronc* function. Second, in contrast to lysates from hemocytes, whole larval lysates were not defective for DEVDase activity (Chew et al., 2004). Together, these findings argue that distinct, tissue specific pathways of effector caspase activation exist in *Drosophila*, some of which are Dronc-dependent and some of which are Dronc-independent.

In wandering third instar larva, *dronc*⁵¹ animals often exhibit abnormalities of internal structures. For example, the wing discs of these mutants are typically deformed and larger than wild type counterparts (Figure 2.7). Others in the lab examined hemocytes in 3rd instar larva and discovered a conspicuous hyperplasia of blood cells in *dronc*⁵¹ animals (Chew et al., 2004). To facilitate quantitative assessments of this

phenotype, hemocytes were labelled with green fluorescent protein (GFP) using the Hml-GAL4:UAS-GFP marker chromosome. When I visualized hemocytes with this marker *in vivo*, *dronc*⁵¹ animals show radical hyperplasia of blood cells at the wandering 3rd-instar larval stage (Figure 2.4). In animals homozygous for the Hml-GAL4:UAS-GFP marker chromosome, about half of all hemocytes are negative for GFP and it is possible that GFP⁺ hemocytes were amplified at the expense of GFP⁻ hemocytes. However, flow cytometry studies (as in Figure 2.2) established that the ratio of GFP⁻ to GFP⁺ hemocytes is unaffected in *dronc*⁵¹ (not shown). Therefore, elevated blood cell numbers in *dronc*⁵¹ larva derive from absolute increases in cell number, rather than redirected fates among hemocyte subpopulations labeled here.

***dronc* is required for fine patterning of the adult eye**

Because *dronc* mutants are late 3rd instar larval-early pupal lethal, we used a FLP-FRT based recombination strategy (Stowers and Schwarz, 1999) to produce eyes made exclusively from *dronc*⁵¹ homozygous cells (see methods) to examine requirements for the action of *dronc* in the formation of adult tissues. Our strategy was authenticated, in part, by the appearance of rare individuals where only one of two eyes underwent FLP-induced recombination (Figure 2.5D). At the gross level, *dronc*⁻ eyes

had normal size and overall structure but, at a finer scale, these showed a 'rough' phenotype (Figure 2.5C) when compared to wild type (Figure 2.5A) and FLP/FRT controls (Figure 2.5B). This defect indicates that loss of *dronc* somehow disrupts normal developmental patterning. We can exclude extra photoreceptor cells and/or abnormal ommatidial size as the basis for this phenotype, since these features appeared normal in plastic sections of *dronc*⁻ eyes (not shown). Therefore, it is likely that cell types not examined here are affected.

The Dronc/Dark axis is required for proper maintenance of adult wing tissue

To further examine *dronc* function in the formation of adult tissues, we produced *dronc*⁵¹ clones in the wing (see Methods). At eclosion, adult wings mosaic for *dronc*⁵¹ were morphologically normal and indistinguishable from wild type. Therefore, *dronc* function is not required for normal formation of wing tissue. However, within 4 days, melanized blemishes appeared at random positions throughout the wing of all mosaic animals (Figure 2.6A and 2.6B). Although wing abnormalities are hardly uncommon, to our knowledge, all previously described wing phenotypes are congenital (existing at eclosion). Therefore, the progressive and age-dependent nature of these blemishes is quite novel. Additional

significance can be assigned to this phenotype because similar, yet less severe, wing blemishes are also observed in adults homozygous for *dark^{CD4}*, which is a hypomorphic allele of the Apaf-1/Ced4 counterpart (Chew et al., 2004), (Rodriguez et al., 1999).

Defect in exit from cell cycle arrest in *dronc* mutants after ionizing radiation (IR)

Recently *dronc* was implicated in compensatory proliferation (Huh et al., 2004b; Ryoo et al., 2004). Compensatory proliferation means that dying cells send proliferation signals to neighboring cells to compensate for their removal (Huh et al., 2004b). We tested the affect of Dronc on cell proliferation dynamics after IR treatment of larval wing discs (Figure 2.7). Wing discs from 3rd instar larvae were radiation treated and stained for phosphohistone H3 (Brodsky et al., 2004; Sogame et al., 2003). Phosphohistone H3 antibody detects cells in mitosis, and thus it is a measure of mitotic index. Because both *dmp53* (Sogame et al., 2003) and *dronc* (Chapter 3, Figure 3.6) prevent cell death upon IR treatment, to exclude the cell death effect, *dmp53* was used as a control. It has been reported previously that *dmp53* is not required for the radiation-induced cell cycle arrest (Ollmann et al., 2000; Sogame et al., 2003). Similarly, we did not see a difference in cell proliferation dynamics between yw and

dmp53 discs at different time points. But *dronc* mutants displayed significant delay in exit from the cell cycle arrest (Figure 2.7). In *dronc* mutants after IR treatment, the mitotic index did not show full rescue of mitosis to uninduced levels even 13 hr later. Therefore, Dronc plays a role in cell proliferation upon the genotoxic stress besides apoptosis.

Discussion

Our results establish that *dronc* profoundly governs apoptotic responses among mature blood cells. In fact, this apical caspase dictated sensitivities to a surprisingly broad range of insults, from widespread changes in translation (Cycloheximide) or transcription rates (Actinomycin D) to the likely focal impact of a small molecule Smac mimetic (Li et al., 2004). In addition, *dronc*⁻ cells were completely insensitive in a model of genotoxic stress caused by Topoisomerase inhibition (etoposide). Therefore, like *caspase-9* in mammals (Zheng et al., 1999), multiple signaling networks must ultimately converge upon this apical caspase. It is especially noteworthy here that *dronc*⁻ cells were also resistant when challenged by 1% ethanol (Table 2.1). Since mechanisms of cell death in response to alcohols are largely unknown, continued studies in this model could highlight unique pathways connecting alcohol exposure and caspase activity.

dronc mutations also share supernumerary cells in common with mutants at *dark* (Rodriguez et al., 1999). From our studies thus far, hyperplasia of hematopoietic cells is among the more striking and unanticipated *dronc*⁵¹ phenotypes. Our results demonstrate that *dronc* is a fundamental regulator of blood cell number but they do not fully establish the sources of dysregulation. Since *dronc*⁻ hemocytes are inherently

resistant to apoptosis (Figures 2.1-3, Table 2.1) it seems likely that autonomous failures in PCD contribute to this phenotype.

Our analyses of mosaic tissues also exposed unanticipated roles for this caspase in the preservation and/or fine scale patterning of adult tissues. Wings chimeric for *dronc* were grossly normal at eclosion and, therefore, *dronc* is not essential to form this tissue. It is also worth noting that, to our knowledge, the progressive nature of the adult wing phenotype shown in Figure 2.6 is novel and, consequently, the pathology responsible for this age-dependent defect is intriguing. One possible explanation may involve epidermal cells of the wing, which are effectively removed by PCD hours after eclosion (Kimura et al., 2004). Perhaps without proper *dronc* activity, failures in this process lead to persisting patches of cells that become hypoxic and melanized over a period of several days. This interpretation turns out to be correct as recently shown by others in our lab (see Chapter 3, Future Directions).

Retinal tissues produced exclusively from *dronc*⁻ cells offer different, but equally informative lessons. Since adult eyes lacking this caspase were grossly normal, we can exclude a requirement for *dronc* as an arbiter of overall size and structure in the formation of these organs. Given its insensitivity to the general inhibitor p35 (Hawkins et al., 2000; Meier et al., 2000b) and recently proposed nonapoptotic roles for this

caspase in spermatid individualization (Huh et al., 2004b) and compensatory proliferation (Huh et al., 2004a), we emphasize that neither of these outcomes were obvious or predictable. Equally noteworthy, however, was a characteristic 'rough' phenotype in whole eyes formed without *dronc*, which implicates important roles for this caspase in pattern formation at a finer scale.

Recent findings indicate functions of *dronc* unrelated to PCD such as spermatid individualization (Huh et al., 2004b) and compensatory proliferation (Huh et al., 2004a). *Dronc* mutant wing discs display a defect in exit from cell cycle arrest after IR treatment. We can assign this affect of *dronc* to its other function(s) since both *dmp53* and *dronc* mutants prevent the stress-induced cell death. Besides to this, the experiment also demonstrates that *dmp53* does not modify cell cycle arrest in this system at different time points.

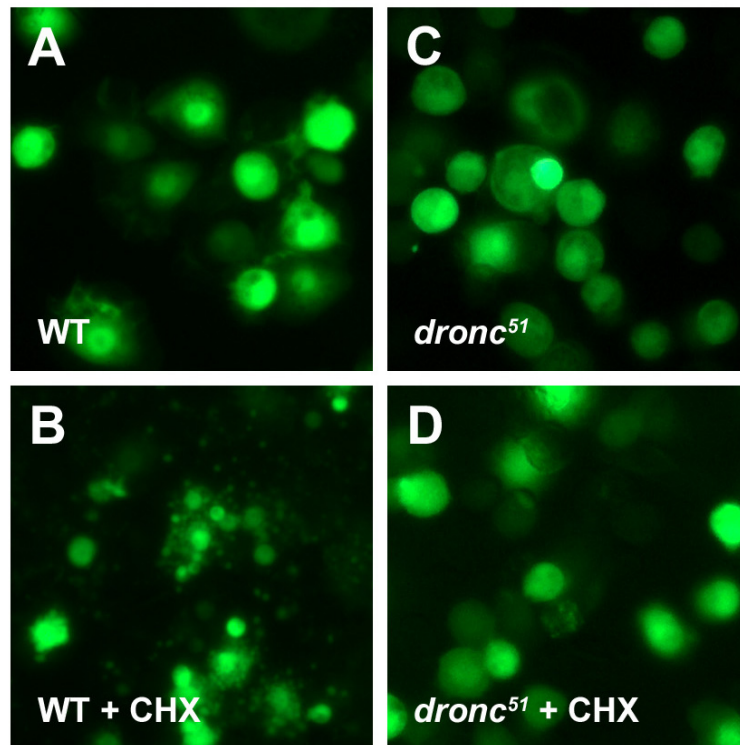


Figure 2.1. *dronc* is required for stress-induced apoptosis. Hemocyte aspirates expressing *Hml-GAL4:UAS-GFP* (a marker chromosome for hemocytes) from wild type and *dronc*⁵¹ larvae were challenged with various chemical stressors *ex vivo*. Cycloheximide (CHX) induced apoptosis is readily seen in wild type cells (compare A and B) but hemocytes from *dronc*⁵¹ animals are insensitive to this challenge (compare C and D).

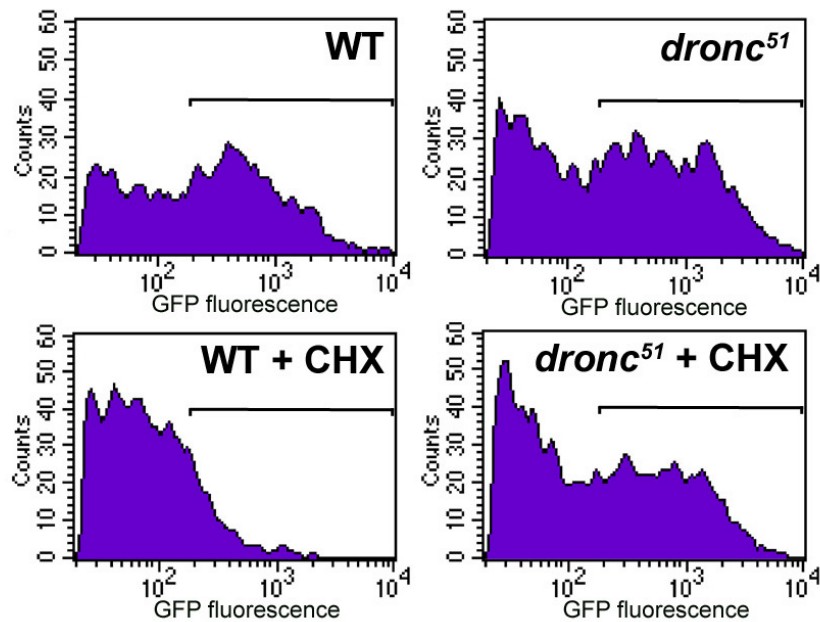


Figure 2.2. Stress resistance of *dronc* mutant hemocytes confirmed by flow cytometry. Hemocyte aspirates expressing *Hml-GAL4:UAS-GFP* from wild type and *dronc*⁵¹ larvae were treated with CHX and flow cytometric analysis was performed 8 hrs later. Flow cytometric analysis detects CHX induced apoptosis as loss of GFP expressing cells. Brackets denote viable cells. Note loss of this population in wild type but not *dronc*⁵¹ cultures.

Treatment	% Death			
	8 hr		20 hr	
	wt	<i>dronc</i> ⁵¹	wt	<i>dronc</i> ⁵¹
Untreated	2 ± 2	0 ± 9	3 ± 2	0 ± 9
DMSO	3 ± 2	12 ± 6	6 ± 4	(1) ± 4
Cycloheximide	90 ± 2	2 ± 1	92 ± 2	7 ± 8
Actinomycin D	98 ± 2	2 ± 2	ND	6 ± 10
Etoposide	72 ± 6	1 ± 1	71 ± 11	5 ± 3
Ethanol	6 ± 2	13 ± 5	40 ± 12	7 ± 9
Smac mimetic	98 ± 1	4 ± 2	98 ± 1	(1) ± 7

Table 2.1. *dronc* is required for apoptosis induced by broad range of stress stimuli. Quantification of apoptosis at 8hr and 20hr, induced by the various agents, is indicated. Since measures of percent death were normalized to untreated wells, and apoptosis of *dronc*⁵¹ hemocytes is extremely rare, note that cell death counts in *dronc*⁵¹ aspirates arise predominantly, if not exclusively, from variance in plating efficiencies. Percentages shown with standard deviations, and parenthesis denote a negative number.

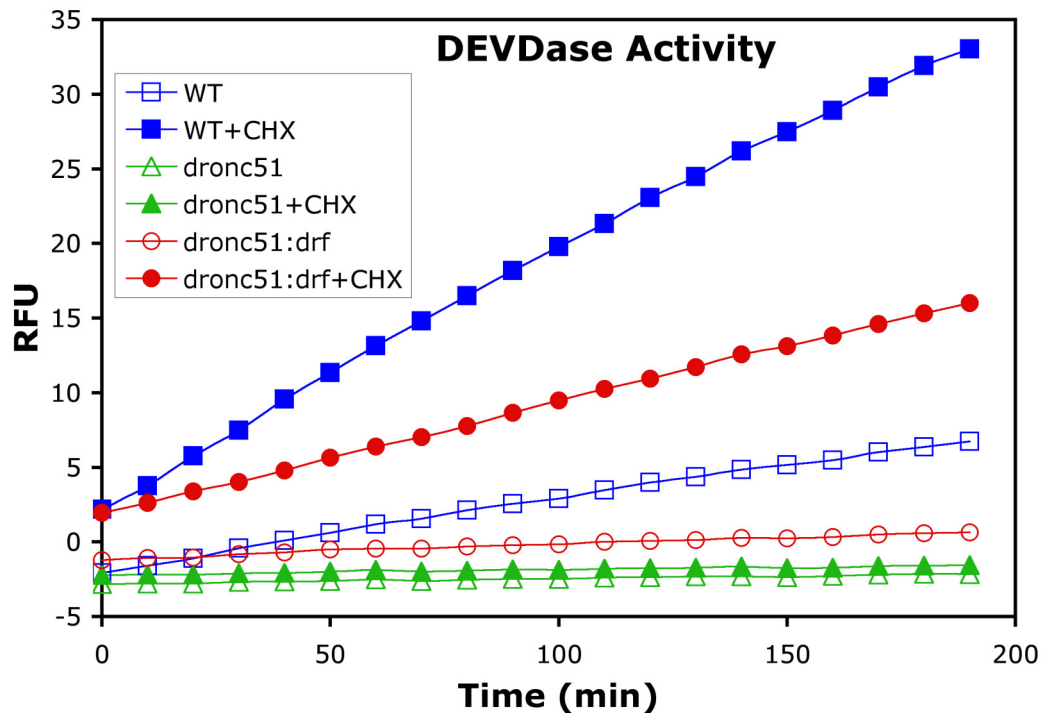


Figure 2.3. *dronc* is required for effector caspase activity. DEVD is a peptide substrate for effector caspases. DEVDase activity of hemocyte lysates derived from larvae of indicated genotypes (treated with or without CHX) was measured. Upon CHX treatment wild type and the *dronc* rescue (drf) hemocytes display increased activity. But no detectable activity occurs in lysates from *dronc*⁵¹ hemocytes under either condition. Also note that hemocytes derived from the *dronc* rescue strain (drf) exhibit ~50% wild type activity. Data shown are representative of multiple trials. RFU, relative fluorescence units.

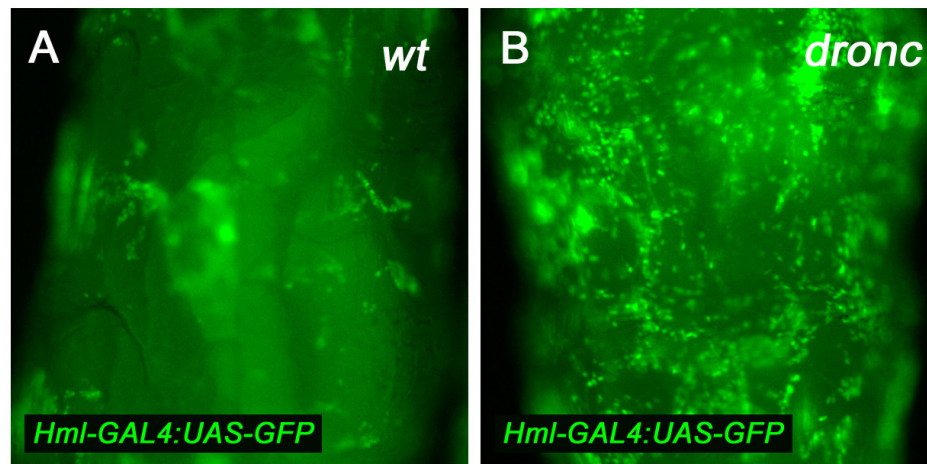


Figure 2.4. Hyperplasia of blood cells in *dronc* mutant animals. Hemocytes were detected using *Hml-GAL4:UAS-GFP*, a marker chromosome for hemocytes. Whole mount wild type (A) and *dronc*⁵¹ (B) wandering 3rd instar larvae showing GFP labeled hemocytes through the transparent body wall. Note that the fluorescence associated with gut is non-specific.

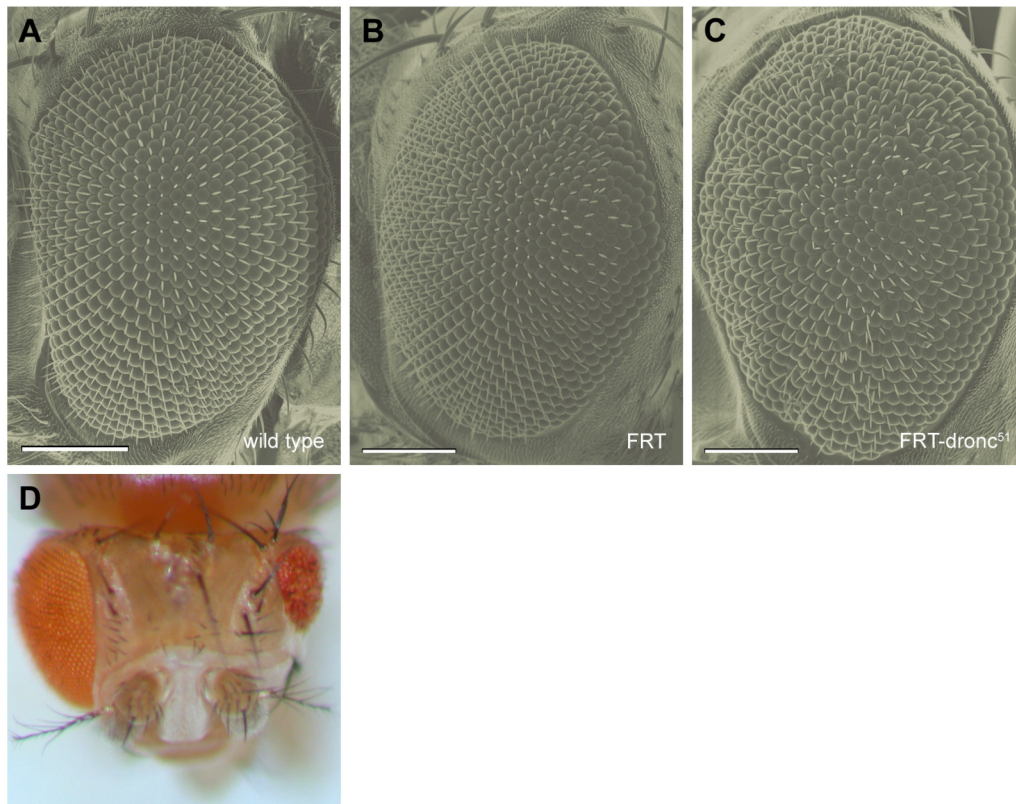


Figure 2.5. *dronc* is required for fine patterning of the retina. Whole eyes lacking *dronc* were produced using *FLP/FRT* recombination together with *eyeless* selection (Stowers and Schwarz, 1999). Scanning electron micrographs of eyes shown are (A) parental wild type control; (B) *FLP/FRT* control and (C) *FLP/FRT-dronc*⁵¹. Note increased 'roughness' in (C) compared to (B). Also note that genotype of animals (see materials and methods) in (B) and (C) are identical except for the *dronc*⁵¹ chromosome arm. (D) Example of rare animal where only one eye (larger) underwent mitotic recombination, but the other eye did not.

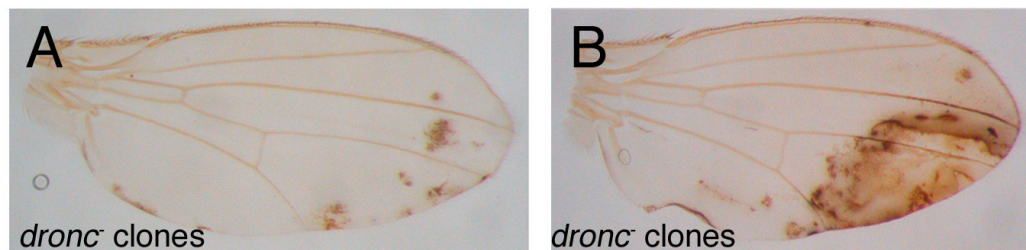


Figure 2.6. Wings mosaic for *dronc* display black blemishes. Both wings are mosaic for *dronc*⁵¹. Genotype is *vg:flp/+; dronc*⁵¹, *FRT79/FRT79* (see materials). Note that wings are normal at eclosion and blemishes appear after 4 days. Pictured here are wings at 7 days.

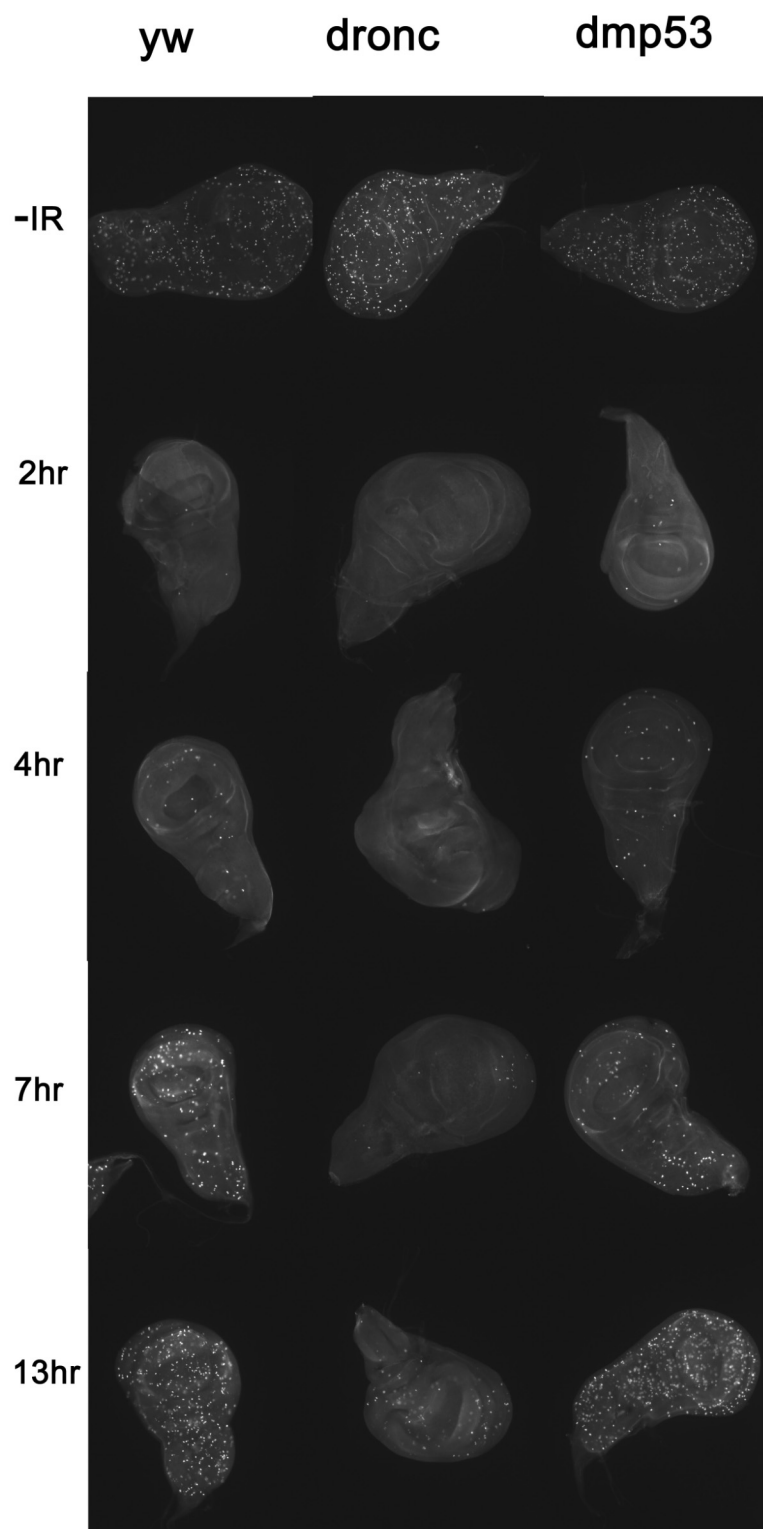


Figure 2.7. Delayed exit from cell cycle arrest in *dronc* mutants after ionizing radiation (IR). anti-phospho-Histone H3 antibody detects cells undergoing mitosis. *yw*, *dronc* and *dmp53* 3rd instar larval wing discs display similar number of cells undergoing mitosis without IR treatment (top panels). To detect any effect of *dronc* to IR-induced cell cycle arrest or exit from the arrest, the larvae were radiation treated (4kRad (40Gray)), wing discs were dissected and then stained at indicated time points (bottom panels). No significant difference was observed between *yw* and *dmp53*, but *dronc* mutants displayed significant delay in exit from the cell cycle arrest. Actually in *dronc* mutants after IR the mitotic index did not show full rescue of mitosis to uninduced levels even after 13 hr later. At least 12 wing discs were stained for each.

CHAPTER THREE

GENERATION AND FUNCTIONAL CHARACTERIZATION OF *DARK* NULL MUTANT ANIMALS

Abstract

Apical caspases are stimulated upon interaction with adaptor molecules. The adaptor protein Dark, the *Drosophila* homolog of nematode Ced-4 and mammalian Apaf-1, regulates the apical caspase Dronc, through interactions involving respective caspase recruitment domains (CARD). Here I show the generation and functional characterization of dark null mutant animals. Using *in vivo* and *ex vivo* assays, I demonstrate a global apoptogenic requirement for *dark* and show that a required focus of *dark*⁻ organismal lethality maps to the central nervous system. Dark protein itself is a caspase substrate and I found that alterations of this cleavage site produced the first hypermorphic point mutation within the Apaf-1/Ced4 gene family. Finally I show functional similarities of *dronc* and *dark* null mutations.

Introduction

Apical and effector caspases lie at the core of the apoptotic program (Danial and Korsmeyer, 2004). Upon interaction with adaptor molecules, apical caspases are stimulated to activate effector caspases by proteolysis. Dark, the *Drosophila* homolog of nematode Ced-4 and mammalian Apaf-1, is thought to regulate the apical caspase Dronc, through interactions involving respective caspase recruitment domains (CARD) (reviewed in (Mills et al., 2005)).

Three broadly conserved protein families represented by Ced9/Bcl2, Ced4/Apaf1 and Ced3/Caspase 9, define fundamental components in pathways of caspase control. However, a unified mechanism for their action in cell death remains elusive since analogous physical interactions seen between nematode Ced9 and Ced4 do not occur among orthologous mammalian counterparts (Moriishi et al., 1999). Instead, mammalian Bcl2 proteins indirectly engage Apaf1 by controlling mitochondrial release of cytochrome c, which promotes formation of a multimeric complex referred to as the apoptosome (Danial and Korsmeyer, 2004; Spierings et al., 2005). While the fly counterparts of these genes add provocative clues, particularly with respect to negative regulators of caspase activity (Salvesen and Abrams, 2004), they also complicate the picture, since cytochrome c appears dispensable for

Drosophila Apaf-1 (*Dark*) dependent cell death despite conservation of a WD domain thought necessary for cytochrome c binding and regulation (Adrain et al., 1999; Dorstyn et al., 2004; Hu et al., 1998; Rodriguez et al., 1999; Zimmermann et al., 2002). Previous data from us and others on viable hypomorphic alleles (Kanuka et al., 1999; Rodriguez et al., 1999; Zhou et al., 1999) established that *Dark* shares functional properties with counterparts in *C. elegans*, where Ced-4 is required for all PCD, and in the mouse, where context-specific apoptogenic requirements for Apaf-1 are seen. However, central questions approachable only with a null allele, remained open. Another aim of this study is to find out whether there are different functions of *Dark* and *Dronc*.

Here I isolate a single-gene null mutation at *dark* and demonstrate a general requirement for this gene in PCD and stress-induced apoptosis. The role for *dark* in PCD was not absolute, however, since rare cell deaths were observed. We show that a required focus of *dark*⁻ organismal lethality maps to the central nervous system and also describe the first hypermorphic allele within the Apaf-1/Ced4 gene family.

Materials and Methods

Generation of *dark* null mutation. Antony Rodriguez has initiated mutagenesis of *dark* by P-element imprecise excision and I was involved in the initial identification of the mutants. Using RT-PCR it was shown by Antony that *dark*⁸² strain does not have *dark* transcript. Later, I characterized and validated the deletion by using genomic PCR across the deletion junction. The PCR product across the deletion junction was sequenced. For genomic PCR following primer pair was used, primers specific to *dark* and the P-element, (primers 1 and 2, see Figure 3-1A,B):
 1: 5'-GCCGACGGGACACCTTATGTTATTTTCATC -3', 2: 5'-TGCAAGCTCGCGATTTTGCCATTGACGAGCGTG-3'. Genomic PCR and RT-PCR were performed as in (Chew et al., 2004) with the relevant gene specific primers.

Strains. A GFP-labeled balancer was used to genotype 3rd instar larvae, *dark*⁸²/ CyO, actin-GFP. In order to make conditional mutants of *dark*, FRT42D was recombined with *dark*⁸² (by Antony Rodriguez). The method for producing wing clones was as in (Vegh and Basler, 2003). *vg:flp*, FRT42D/ *dark*⁸² FRT42D refers to *Vg-GAL4:UAS-FLP*, FRT42D/ *dark*⁸², FRT42D. *dark* transgenes were prepared by Po Chen.

Germline Clones and AO Staining. The *dark*⁸² allele was recombined onto the FRT^{2R-G13} chromosome. To generate *dark*⁸² maternal-null embryos, the Dominant Female Sterile (DFS) technique was used as described previously (Chou and Perrimon, 1996). *hs-Flp/+ ; OvoD FRT^{2R-G13} / dark⁸² FRT^{2R-G13}* females were crossed with *dark*⁸²/ CyO, actin-GFP males to generate maternal and zygotic dark null embryos. To detect cell death, Acridine Orange (AO) staining was performed as in (Abrams et al., 1993).

Wing Cell Death Assay. Acridine Orange staining of wing discs after ionizing radiation (cell death assay) was performed as described previously in (Brodsky et al., 2000a).

Ex Vivo Hemocyte Analyses. Wandering L3 instar larvae were prepared as in Chapter-2, with the following modifications. Hemolymph was collected from six larvae and agents were added after media addition. Membrane blebbing, a characteristic feature of apoptosis, was used to quantify apoptosis. At ~6 hr post treatment cells were stained with a fluorescent membrane dye, 10 uM CellTracker (Molecular Probes) in DMSO, to facilitate visualization of apoptotic membrane blebbing (without

fluorescent labeling it was difficult to assess membrane blebbing due to phagocytic nature of hemocytes).

Hemocyte Counts. Wandering L3 instar larvae were prepared as above. 1 ul of hemolymph collected from six larvae is mixed with 19 ul PBS and the fluorescent membrane dye, 10 uM CellTracker (Molecular Probes). Then cells were counted with hemacytometer. For each genotype at least four different countings were conducted.

Ovary and testis staining. DAPI staining of ovaries and testes is performed as in (Goldstein and Fyrberg, 1994) and Zeiss LSM 510 META laser scanning confocal microscope was used to take pictures.

Imaging and Microscopy. Please see Chapter 2.

Results

***dark*⁸² is null allele**

To investigate molecular genetic properties of the *Drosophila* apoptosome, and illuminate possible ‘non-death’ roles for this gene in development, we recovered a null mutation at *dark* in a screen for excision derivatives of an existing P insertion (Rodriguez et al., 1999). *dark*⁸² is a 6.3kb deletion spanning the entire open reading frame and nearly the entire transcription unit (Figure 3.1A-C). Animals homozygous for this allele arrest as late pupae and often present a characteristic dark blister located centrally along the midline. The mutation fails to complement all existing hypomorphic *dark* alleles and also complements flanking genes (see methods). In addition, homozygous *dark*⁸² animals were rescued to viability using a transgene containing a full-length *dark* cDNA (see Table 3.1). Hence, *dark*⁸² is a lethal, single-gene null mutation.

Elimination of maternal and zygotic *dark*

Since animals homozygous for *dark*⁸² survive to pupation, I used the Dominant Female Sterile technique to examine phenotypes of animals lacking maternally supplied *dark* (see methods). I found normal PCD patterns in embryos that retained zygotic but lacked maternal *dark* (Figure

3.2A-B). In contrast, embryos devoid of both maternal and zygotic *dark* were almost entirely cell death defective, with rare cell deaths noticeable in later staged animals (Figure 3.2C-D). These observations demonstrate a global need for *dark* in PCD. However, the requirement is not absolute since occasional apoptotic cell deaths did occur in the complete absence of *dark* function. Embryos lacking maternal and zygotic *dark* failed to hatch and were also defective for head involution, similar to cell death defective mutations in the *Reaper* region (Grether et al., 1995; White et al., 1994) and *dronc* (Chew et al., 2004). At the same time, gastrulation, segmental patterning and extension of the germ band appeared grossly normal in the absence of *dark*. Hence, to the extent that these events involve migration and/or movement (Geisbrecht and Montell, 2004), we note that the proposed role for *dark* in cell motility evidently does not generalize to these morphogenic processes.

I also tested larval hemocytes in *ex vivo* models of stress-induced cell killing (Figure 3.3A-C). To facilitate the analysis I have developed an assay to label cells (see methods), by which we do not have to genetically label hemocytes. In contrast to wild type counterparts, *dark*⁻ hemocytes were completely resistant to a smac mimetic, which antagonizes inhibitor of apoptosis proteins (IAPs) and is thought to simulate the action of *reaper* proteins (Li et al., 2004; Salvesen and Abrams, 2004). Likewise, *dark*⁻

cells were completely insensitive to the apoptogenic effects of cycloheximide, a protein synthesis inhibitor. In this respect *Dark* functions same as *Dronc* (Figure 2.1-3). I used the same technique to analyze *dredd* (a caspase) and *debcl* (a Bcl-2 gene) mutant hemocytes. Contrary to *dronc* and *dark* hemocytes, they did not display resistance to the death stimuli (not shown). Together, these data establish a central role for the action of *dark* in programmed and unprogrammed apoptosis.

Tissue-specific restoration in the CNS reverses *dark* lethality

To confirm and extend these studies, we restored *dark* using a transgene (designated UAS-*dark*^{WT}) that places a full-length cDNA under the control of the yeast derived UAS promoter, which permits conditional expression when combined with tissue specific “Gal4 driver” strains. Table 1 shows that, in two independent transformed lines, ubiquitous expression of wild type *dark*, using either Tubulin-Gal4 or Daughterless-Gal4 drivers, completely rescued *dark*⁸² lethality. In parallel studies, expression of UAS-*dark*^{WT} in mutant hemocytes (via the Hml-Gal4 driver) did not rescue animal viability but did partially restore sensitivity to smac mimetic killing to these cells (Figure 3.5B). Surprisingly, exclusive restoration of *dark* to the post-embryonic central nervous system using pCNS-Gal4 (also called c81-Gal4) reversed *dark*⁸² lethality but restoration

of *dark* to the embryonic CNS and imaginal discs (c833-Gal4 driver) did not. Although we can not exclude the possibility that maternal *dark* is depleted in the CNS earlier than other tissues, these results demonstrate that, at minimum, expression of *dark* in the post-embryonic CNS is necessary to reverse organismal lethality and produce a viable adult. I also note here that male and female adults rescued by pCNS-Gal4 driven *dark* were sterile. However, in DAPI stained preparations, no associated defects in germ line formation were detected at the gross morphological level (Figure 3.4).

A caspase cleavage site in Dark confers hypermorphic gene activity when mutated

Exploratory *in vitro* studies with recombinant Dark identified a putative caspase cleavage site that was mapped to Asp1292 (Figure 3.5A, Dr Lai Wang's finding). To examine the biologic effects of this site *in vivo*, we tested a variant, *dark^v* (see methods) that substitutes Ala for Asp at position 1292. Like wild type transformants, ubiquitous restoration of this *dark* variant (UAS-*dark^v*) reversed lethality caused by *dark⁸²* (Dr Chen's data) (Akdemir et al., 2006). However, in the absence of any Gal4 driver, 'leaky' expression of UAS-*dark^v* also rescued *dark⁸²* lethality but, surprisingly, wild type *dark* did not. Hypermorphic properties related to

dark^V were also noted in *ex vivo* hemocyte assays (Figure 3.5B). Expression of the wild type cDNA in *dark⁸²* hemocytes only mildly restored stimulus dependent apoptosis after treatment with a Smac mimetic. However, *dark^V* almost completely restored this apoptotic response to *dark⁸²* hemocytes (Figure 3.5B). These results (and others (Akdemir et al., 2006)) are consistent with negative feedback models whereby the action of Dark protein may be directly repressed by effector caspases, thereby setting an apoptotic threshold in cells that are specified for death.

Functional similarities of *dronc* and *dark* null mutations

To find out whether there are different functions of Dark and Dronc, several experiments were performed (Figures 3.6-8). First, when larval wing discs from the null mutants were tested for resistance to ionizing radiation-induced cell death, both mutants displayed complete resistance to this stimulus (Figure 3.6). Therefore, similar to hemocytes, wing discs of *dark* and *dronc* mutants are resistant to the radiation-induced cell death. Secondly, we observed “dark blemishes” in wings mosaic for *dark*, as in *dronc* analysis in Chapter 2 (Figure 3.7). “dark blemishes” form due to the failure of wing epithelial cell death after eclosion (N. Link’s data). We know that there is hyperplasia of hemocytes in *dronc* mutant larvae (Chapter 2 and (Chew et al., 2004)). As shown in Figure 3.8 I did not observe

hyperplasia of hemocytes in *dark* mutant 3rd instar larvae in contrast to *dronc* mutants. Because maternal contribution of these proteins may diminish at different times, we cannot conclude that Dronc has Dark-independent role in controlling hemocyte number.

Discussion

Here I show that *dark* encodes generalized functions in PCD. Loss of maternal and zygotic product caused profound defects, abolishing nearly all apoptotic deaths in the embryo. Likewise, elimination of zygotic *dark* prevented the histolytic death of salivary gland cells (Akdemir et al., 2006) and also reversed drug-induced killing of hemocytes. These results establish widespread functions for *dark* in distinct models of programmed and stress-induced cell death. The role for *dark* in PCD is not absolute, however, since rare apoptotic cell deaths were observed in animals lacking both maternal and zygotic product. Though reminiscent of phenotypes associated with complete deletions in the *Reaper* region, loss of *dark* did not appear to perfectly phenocopy these since occasional apoptotic cell deaths are observed. To substantiate this idea, I carefully compared the incidence of *dark*-independent cell deaths to the rare cell deaths that occur in H99 homozygous embryos. Among animals lacking maternal and zygotic *dark*, an average of 8.9 ± 2.0 cell deaths were found in late embryonic stages. However, only 3.1 ± 2.1 cell deaths were found in comparably staged H99 embryos. Hence, in this respect, animals devoid of *dark* emulate cell death defects seen in animals lacking maternal and zygotic *dronc* (Xu et al., 2005). Together, these observations establish that for a small population of embryonic cells, apoptotic activators in the

Reaper region can specify apoptosis without engaging the fly apoptosome. Similar pathways might occur in post-embryonic stages but I cannot derive firm conclusions in unaffected larval tissues, given caveats relating to perdurance of maternally derived product.

Unlike its counterparts in the worm or the mouse, genetic elimination of *dark* produced a strictly lethal phenotype. Since ubiquitous and cell-type specific expression of a *dark* transgene complemented this phenotype, it was possible to map the focus of genetic activity responsible for restoring viability. We found that *dark*⁸² lethality was reversed when expression was restored to cells of the post-embryonic CNS but complementation failed if *dark* was restored to hemocytes or imaginal discs. These results highlight essential functions for zygotic *dark* in the post-embryonic CNS and suggest that the action of this gene within other tissues may not be necessary for viability. Transgenic complementation also proved to be an effective means for distinguishing wild type gene action from derivatives with altered activities. By this approach, we determined that *dark*^v encodes striking hypermorphic activity (Akdemir et al., 2006) without affecting transgenic expression levels (Po Chen's data). Since *dark*^v is mutated at a caspase cleavage site (Figure 3.5A) the data are consistent with negative feedback models whereby the action of Dark is directly repressed by effector caspases, perhaps setting an apoptotic

threshold in cells that are specified to die. These findings describe the first hypermorphic point mutation among all known alleles in the *ced4/Apaf1* gene family.

Except the hyperplasia of hemocytes in *dronc* mutant 3rd instar larvae in contrast to *dark* mutants, *Dark* and *Dronc* behave similarly in other phenotypes. For instance, animals devoid of both maternal and zygotic *Dark* emulate cell death defects seen in animals lacking *dronc* (Xu et al., 2005). Both mutants are resistant to different stressors: hemocytes to diverse stimuli, wing discs to ionizing radiation. Clonal analysis of both displays blemishes in wings with 100% penetrance due to failure of wing cell death. For difference in hemocyte number, we cannot exclude the possibility of maternal affects.

Future Directions

One of my important findings is that *dronc* and *dark* mutant hemocytes are insensitive to stress-induced apoptosis. In mammalian studies this kind of response was observed in *bax* and *bak* double knockouts (Lindsten and Thompson, 2006; Zong et al., 2004). Based on this finding a genome-wide RNAi screen in our lab by others was initiated to find whether other genes, if any, that when knocked down would show resistance to stress-induced apoptosis. *dronc*⁻ cells were also resistant when challenged by 1% ethanol (Table 2.1) and mechanisms of cell death in response to alcohols are largely unknown. Based on this precedent, others also initiated another RNAi screen in the lab to find genes mediating ethanol-induced death. Continued studies in this model could highlight unique pathways connecting alcohol exposure and caspase activity.

Clonal analysis of *dark* and *dronc* gave “dark blemishes” or “dark spots” in the wing and recently a lab member has demonstrated that these spots were due to undead wing epithelial cells. A modifier screen was performed based on this finding in the lab making use of the easy to score phenotype and the power of clonal analysis. I have also contributed to the design of the screen. Promising modifiers were obtained and they are under investigation in the lab by others.

Since cytochrome c appears dispensable for *Drosophila* Apaf-1 (*Dark*) dependent cell death despite conservation of a WD domain thought necessary for cytochrome c binding and regulation (Adrain et al., 1999; Dorstyn et al., 2004; Hu et al., 1998; Rodriguez et al., 1999; Zimmermann et al., 2002) it remains to be demonstrated how the Dark-Dronc signaling is regulated by diverse signals. Hopefully the screens mentioned above will demonstrate some of the regulators.

Surprisingly DNA-alkylating agents killed *dronc* hemocytes although not through apoptosis (not shown). A similar observation was reported for bax-bak double-mutant mouse embryonic fibroblasts (Zong et al., 2004). My hemocyte culture system would be a valuable tool to test candidate genes that might play a role in signaling this type of damage.

Prevention of cell death in *C.elegans* is not lethal and adults behave normally (Yuan and Horvitz, 2004). Behavioral analysis of *Drosophila* cell death mutants has not been performed. As reported above, CNS expression of Dark rescues *dark* lethality and overexpression of wild type or hyperactive Dark variant does not cause lethality in wild type flies (Po Chen's observation). Also we know from a hypomorphic *dark* mutant (CD4 allele) study that there is hyperplasia of glial cells in larval CNS (Rodriguez et al., 1999). It would be interesting to perform behavioral analysis with CD4 and CNS-overexpressed Dark adult flies.

My data and others indicate that Dronc plays a role in compensatory proliferation. Molecular mechanism of Dronc function in this process remains to be discovered. I speculate that Dronc, similar to Caspase-1, functions in this process by cleaving and mediating secretion of a proliferation factor.

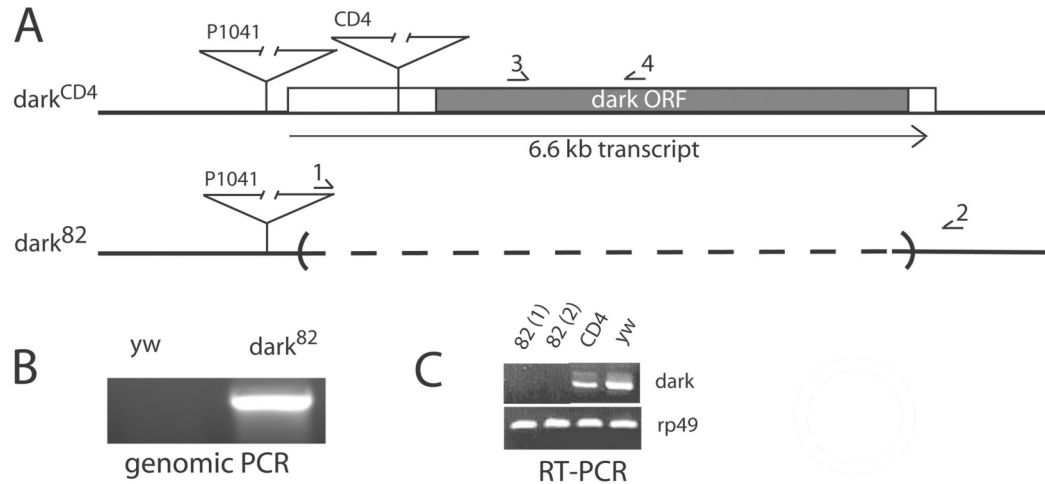


Figure 3.1. Generation of *dark*⁸² null mutation. (A) Schematized view of genomic structure of the *dark* locus, relevant alleles and *dark*⁸² null mutation. The *dark* transcript spans 6.6 kb. *dark*⁸² is a 6,324 bp deletion (dashed line) generated by imprecise excision of the indicated P-element in the *dark*^{CD4} strain (Rodriguez et al., 1999). The allele was mapped by sequencing a 1.3 kb genomic PCR fragment (panel B) using a primer pair (designated 1&2) spanning the junctional interval. In *dark*⁸² sequences from -1277 bp (upstream of the translation start codon) to 19 bp downstream of the stop codon are absent such that the entire *dark* ORF and part of the untranslated 1st exon are missing. Note that 396 bp of sequence from the CD4 transposon remain at this junction. (C) RT-PCR with primer pair 3 and 4, using total RNA from prepupae, confirms complete loss-of *dark* transcript in the *dark*⁸² allele. Two different isolates of *dark*⁸² from the screen were assayed here, 82 (1) and 82 (2). *rp49* is a control. (Contributions: I was involved in screening for *dark* mutants initiated by Antony Rodriguez, and later I have molecularly mapped the mutation.)

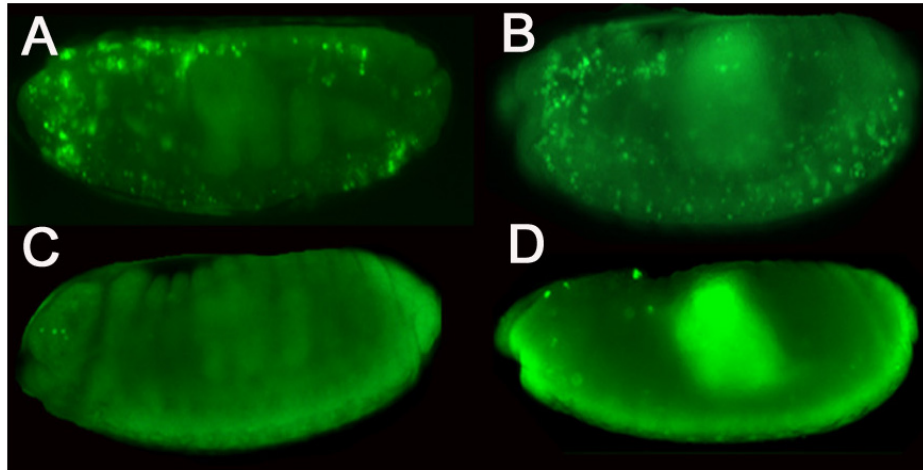


Figure 3.2. *dark* is essential for embryonic programmed cell death (PCD). Maternal and zygotic sources of *dark* were removed using a Dominant Female Sterile strategy (see methods). The resulting embryos lacked nearly all PCD, shown here by Acridine Orange (AO) staining. Panels **A** and **B** show mid-staged embryos eliminated for maternal *dark* but heterozygous for zygotic *dark*. Panels **C** and **D** show comparably staged embryos lacking both maternal and zygotic *dark*. Note that without a source of *dark* function embryos are head involution defective with only few AO positive cells (**C** and **D**).

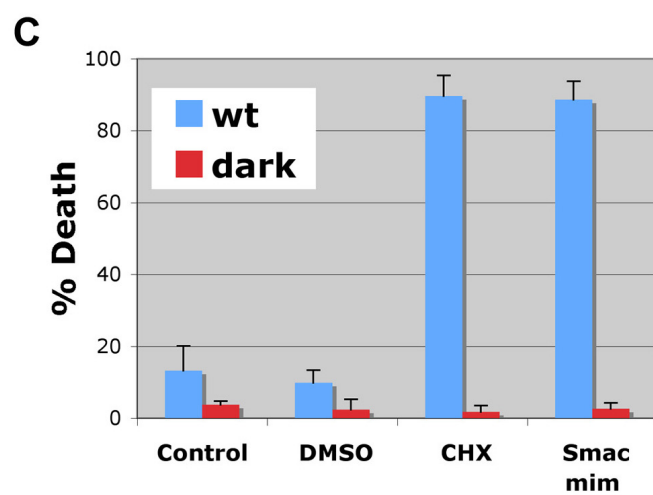
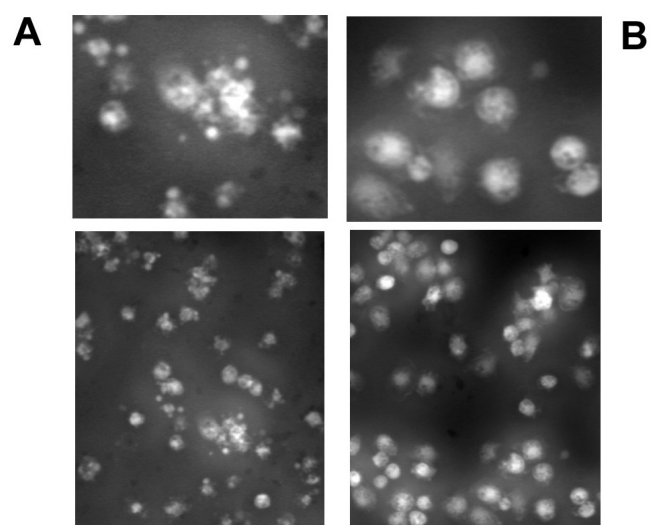


Figure 3.3. *dark* is required for unprogrammed apoptosis.

These panels show a requirement for *dark* in models of stress-induced cell death. Hemocyte aspirates from *dark*⁸² and wild type (*wt*) wandering 3rd instar larvae were treated with chemical stressors *ex vivo* and stained with CellTracker to visualize apoptotic cell blebbing (see methods). Induction of apoptosis in *wt* (**A**) but not *dark*⁸² (**B**) hemocytes is exemplified here with micrographs 6hr after Cycloheximide (CHX) treatment. In panels A and B, top panels are the magnified parts of the bottom panels. (**C**) Quantification of apoptosis 6hr after challenge with either CHX or a smac mimetic (Li et al., 2004) are plotted as the incidence of cell death in percentages. Error bars indicate standard deviations (s.d.).

	Driver	% of rescued <i>dark</i> ⁸² homozygous flies
UAS- <i>dark</i> ^{WT} .H4	No	0% (27)
UAS- <i>dark</i> ^{WT} .B6	No	0% (24)
UAS- <i>dark</i> ^{WT} .H4	Tubulin-Gal4	100% (27)
UAS- <i>dark</i> ^{WT} .B6	Tubulin-Gal4	95% (38)
UAS- <i>dark</i> ^{WT} .H4	Dal-Gal4	100% (34)
UAS- <i>dark</i> ^{WT} .B6	Dal-Gal4	96% (25)
UAS- <i>dark</i> ^{WT} .H4	Hml-Gal4	0% (22)
UAS- <i>dark</i> ^{WT} .B6	Hml-Gal4	0% (33)
UAS- <i>dark</i> ^{WT} .H4	pCNS-Gal4 (c81)	16% (62)
UAS- <i>dark</i> ^{WT} .B6	pCNS-Gal4 (c81)	18% (80)
UAS- <i>dark</i> ^{WT} .H4	c833-Gal4	0% (23)
UAS- <i>dark</i> ^{WT} .B6	c833-Gal4	0% (25)

Table 3.1. CNS-specific rescue of *dark*⁸² lethality by the expression of wild- type *dark* allele.

Data from transgenic rescue experiments is summarized here. Reversal of *dark*⁸² lethality was scored in contexts where tissue specific expression of a wild- type transgene (UAS-*dark*^{WT}) was tested. The left-hand column indicates the transgene tested in combination with the tissue ‘driver’ listed in the middle column. In each case, a single dose of the *dark* transgene and driver are tested. The right-hand column indicates the percent of rescued animals relative to the expected Mendelian value, listed in parentheses. Note that two independent lines were tested (H4 and B6 for UAS-*dark*^{WT}). *dark*⁸² lethality is fully rescued if UAS-*dark*^{WT} is driven by Tubulin-Gal4 or by Dal-Gal4, which both confer ubiquitous expression. In contrast, no rescue is observed if UAS-*dark*^{WT} is combined with an embryonic CNS/larval disc driver (c833-Gal4) or a hemocyte specific driver (Hml-Gal4). However, substantial rescue of *dark*⁸² lethality occurs when expression of UAS-*dark*^{WT} is restored in the post-embryonic CNS using the pCNS-Gal4 driver (also called c81-Gal4) and expressed diffusely throughout brain lobes but not in embryos, egg chambers or imaginal discs (Drapeau et al., 2003; Manseau et al., 1997). (Contributions: Po Chen generated the transgenes, idea to test for CNS rescue was mine, and we both generated the rescue data.)

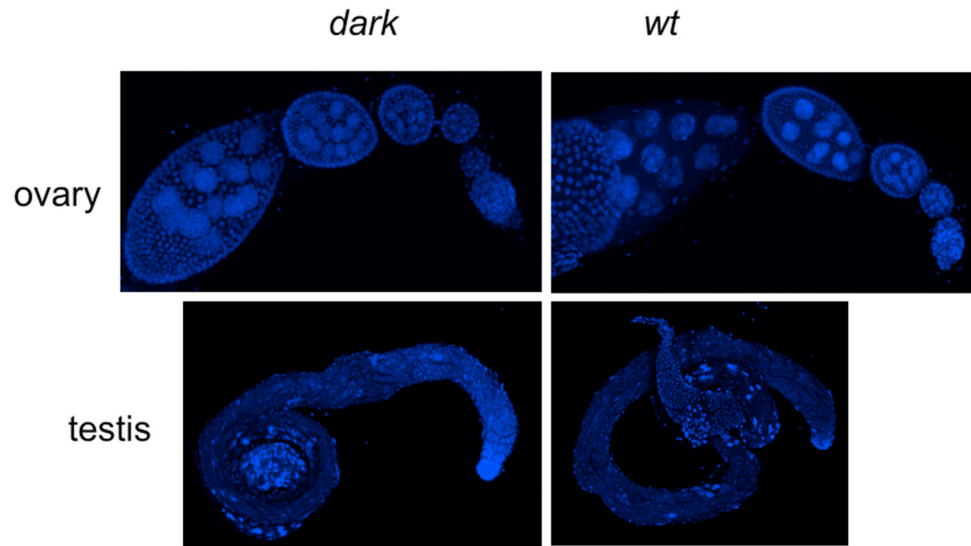


Figure 3.4. Normal gross morphology of germline of the CNS-rescued *dark*⁸². DAPI staining of ovaries and testes is performed and confocal microscopy was used to take pictures (see Table 3.1. for “CNS-rescued *dark*⁸²”). Germline stem cells reside at the tip of the organs (right side) and they differentiate into eggs or sperms. Sperms are motile (data not shown).

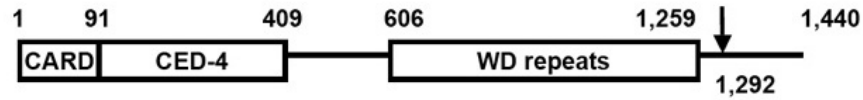
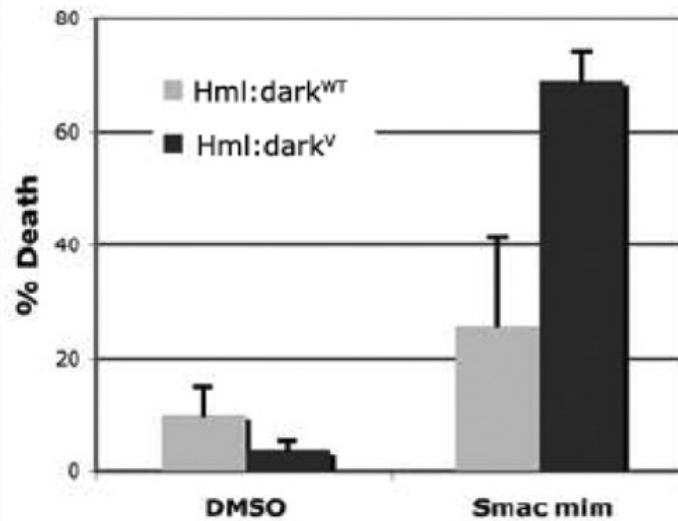
A**B**

Figure 3.5. Alteration of a caspase cleavage site produces a hypermorphic Dark variant.

(A) A cleavage site was identified in Dark (Akdemir et al., 2006). Schematized domain structure of Dark protein and the cleavage site at residue 1292 is shown (arrow). **(B)** Hemocyte aspirates from *dark⁸²; Hml-Gal4:UAS-dark^{WT}* (*Hml:dark^{WT}*) and *dark⁸²; Hml-Gal4:UAS-dark^V* (*Hml:dark^V*) L3 larvae were treated with DMSO or the Smac mimetic (Li et al., 2004), a potent apoptotic inducer. Expression of *UAS-dark^{WT}* in *dark⁸²* hemocytes only mildly restored apoptosis after Smac mimetic treatment. However, *UAS-dark^V* almost completely restored this apoptotic response to *dark⁸²* hemocytes.

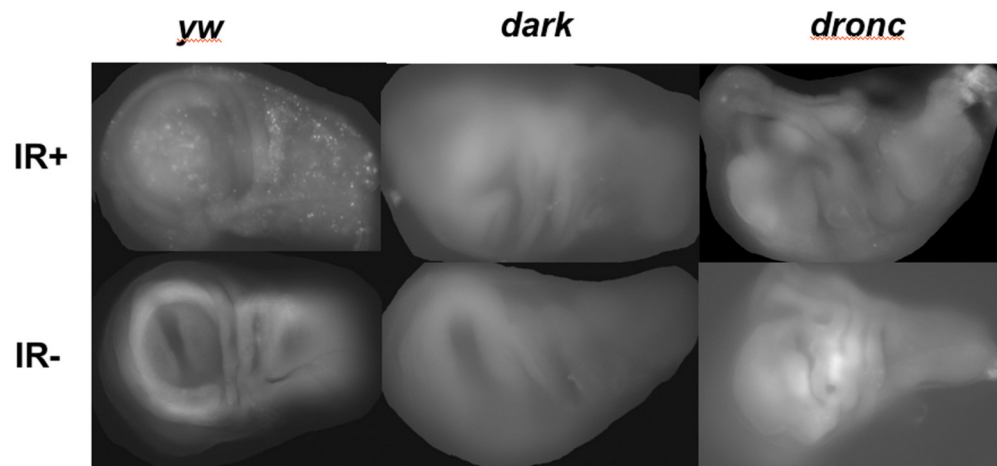


Figure 3.6. *dark* or *dronc* mutants display resistance to ionizing radiation (IR)-induced apoptosis. 3rd instar larvae were mock treated (IR-, bottom panels) or irradiated (IR+, top panels) with 4 kRads. About 4 hr after irradiation apoptotic cells in wing discs were detected by using a vital dye, acridine orange. *yw* discs display AO positive cells after the treatment but neither *dark* nor *dronc*.

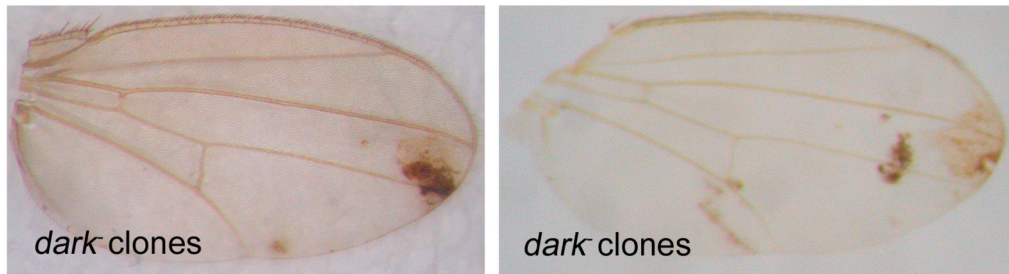


Figure 3.7. Similar to *dronc*, wings mosaic for *dark* display black blemishes. Two different examples of *dark*⁸² mosaic wings. Genotype is *vg:flp*, *FRT42D/ dark*⁸² *FRT42D*. Note that wings are normal at eclosion, blemishes appear after about 4 days. Pictured here are wings at 7 days. Even though expressivity may change, the phenotype is 100% penetrant.

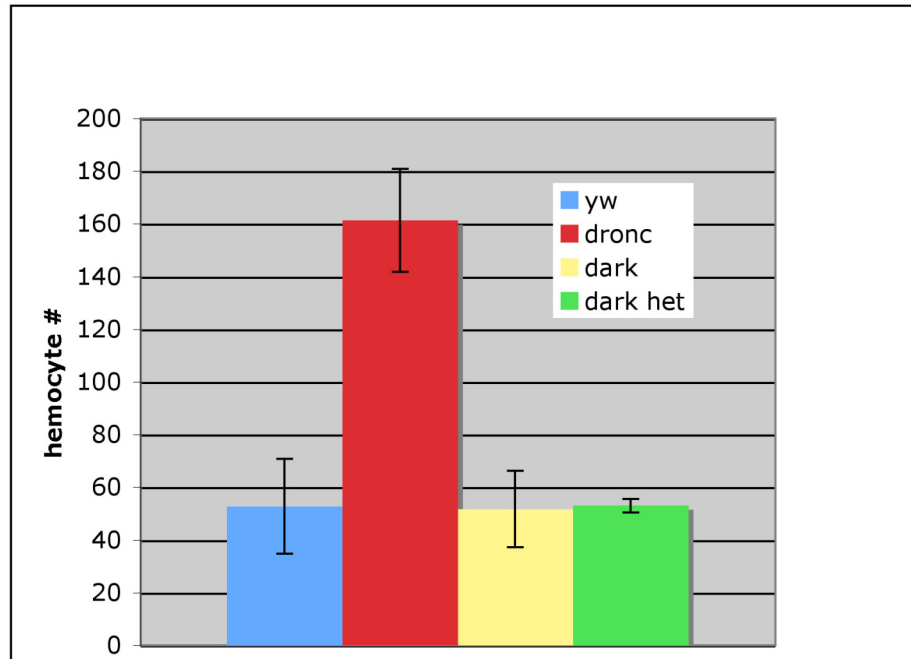


Figure 3.8. Contrary to *dronc* mutants, absence of hyperplasia of blood cells in *dark* mutant animals. Plotted are the hemocyte numbers per unit of hemolymph from indicated genotypes. Hemocytes from wandering 3rd instar larvae were stained with CellTracker, a membrane dye, and counted. For each genotype at least four different counting was performed. Note the increase of hemocyte number in *dronc* mutant animals but no change in *dark* mutants. Error bars, SD.

CHAPTER FOUR

A NOVEL RADIATION RESPONSIVE GENE, *XRP1*, INHIBITS CELL PROLIFERATION AND MAINTAINS GENOMIC STABILITY AFTER EXPOSURE TO GENOTOXIC STRESS

Abstract

Treatment of cells with DNA-damaging agents upregulates many genes, many of which are not functionally characterized. Here we identify and characterize an ionizing radiation (IR)-induced gene, CG17836, designated as *xrp1*. *Xrp1* is robustly responsive to IR, and as inferred from domain structure it is a nuclear protein with DNA-binding activity. We have characterized two different loss-of-function mutants of *xrp1*. In a loss-of-heterozygosity (LOH) assay *xrp1* mutant animals display higher genomic instability than wild types after IR challenge. Even though *xrp1* is not required for apoptosis or cell cycle arrest after IR treatment in animals, surprisingly, its overexpression in cell culture prevents cell proliferation. Thus, *Xrp1* might maintain genomic stability by modulating proliferation capacity upon IR exposure.

Introduction

Different agents constantly damage DNA by causing base damage or the breakage of the phosphodiester bond. Responses of cells to DNA damage are studied extensively in part because of the fact that we exploit DNA damage to cure cancer. Also, loss of maintenance of DNA integrity enables cells to acquire capabilities for malignancy (Gudkov and Komarova, 2003; Hanahan and Weinberg, 2000; Kastan and Bartek, 2004). Many chemotherapeutic drugs and radiation therapy damage DNA. Ionizing radiation (IR), used for radiation therapy, damages DNA mainly by inducing DNA double-strand breaks (Coates et al., 2004; Gudkov and Komarova, 2003).

Cellular responses to DNA damage (eg by IR) include DNA repair systems, cell cycle arrest and apoptosis (Brodsky et al., 2000a). For different types of DNA lesions there is a variety of DNA repair mechanisms. Although not necessarily perfect, if the damage is adequately repaired, the damaged cell will be normal. If it is misrepaired or not repaired, the genetic change will be passed to the descendant cells. Damaged cells inhibit cell cycle progression through cell cycle checkpoints to give more time to the repair mechanisms to function. If the damage is

irreparable then the cell might initiate cellular suicide program, apoptosis (Brodsky et al., 2000a; Friedberg, 2003; Kastan and Bartek, 2004). Therefore, cells have multiple mechanisms to maintain genomic stability in normal or stressed situations.

The p53 tumor suppressor protein is a key player of cellular responses to DNA damage (Brodsky et al., 2000a; Gudkov and Komarova, 2003; Sogame and Abrams, 2003; Sogame et al., 2003). Upon activation by DNA damage p53 “guards the genome” by promoting DNA repair and arresting cell cycle or eliminating the damaged cells by apoptosis in mammals. The importance of p53 is reflected by loss of its function in most human malignancies. Regulation of transcription is the primary mechanism of action of p53 and most mutations in human cancers map to its DNA-binding domain.

In *Drosophila*, p53 is activated by chk2 phosphorylation which itself is activated by ATM/ATR upon irradiation (Brodsky et al., 2000c; Brodsky et al., 2004; Peters et al., 2002). Identification of transcriptional targets of mammalian p53 has been a major focus of p53 research. p21 is a p53 target regulating G1/S transition. Apoptotic targets of p53 include *fas/apo1*, *noxa* (Oda et al., 2000), *puma* (Nakano and Vousden, 2001; Yu et al., 2001) and *bax* (Rong et al., 2002). Some of DNA repair components also are regulated by p53 (Brodsky et al., 2004). Similar to mammalian

p53, *Drosophila* p53 (dmp53) induces apoptosis after radiation treatment but in contrast, it is not required for cell cycle arrest in imaginal discs (Ollmann et al., 2000; Sogame et al., 2003).

Deletion of a genomic region in *Drosophila*, H99, prevents all programmed cell death during development (White et al., 1994). The region encodes to several proapoptotic genes. Reaper is one of them and its expression is induced by ionizing radiation in a dmp53-dependent manner. Dmp53 binds to 20-bp radiation responsive element of reaper (Brodsky et al., 2000a).

To identify the genes that are induced by ionizing radiation similar to reaper (Nordstrom et al., 1996; White et al., 1994), a screen with enhancer trap lines was initiated. The P-element P1569, inserted in CG17836 locus, was robustly responsive to IR. Domain structure of the corresponding protein (with nuclear localization sequence, an HMG motif and a possible bZIP domain) indicates potential DNA-binding activity. After confirming its IR response in different systems we have decided to characterize CG17836 gene. Our hypothesis was that CG17836 plays a role in cellular responses to DNA damage. Here we show the characterization of two different loss-of-function mutations of CG17836. In a loss-of-heterozygosity (LOH) assay, CG17836 mutant animals display higher genomic instability than wild types after IR treatment. CG17836

mutants do not modify apoptosis in several cases that we tested. Even though CG17836 is not required for cell cycle arrest after IR treatment, surprisingly, its overexpression prevents cell proliferation.

Materials And Methods

Stocks. We obtained a deletion strain in the *xrp1* locus, J3E1 that was recovered but not molecularly characterized by Mathew et al (Mathew et al., 2002). A synthetic *xrp1* mutation (Df(3R)Exel6181 / Df(3R)Exel6182) was generated by using Exelixis deletions (Df(3R)Exel6181 and Df(3R)Exel6182) in trans.

Cloning of Xrp1 (CG17836). The longest ORF (RB, Flybase) of *xrp1* was amplified by using One-Step RT-PCR kit (Invitrogen) with a primer pair (sense 5'-GAGCCAGCACGAGTACAGGCGGCACCCACATTCGA , antisense 5'-AGCACTTACGTTAAGCAGGAGCAGGACTGAA) which have BglII restriction sites at 5' ends. The full-length Xrp1 was cloned into the BamHI site of pBluescriptII SK(-) vector and sequenced. The BamHI insert was then subcloned into the BamHI site of pMTAL vector to produce pMTAL-Xrp1. Technicians in the lab carried out the experiments.

Cell Culture. Transient transfection of S2 cells was performed as in (Nordstrom et al., 1996). Basically in 6-well plates S2 cells were plated at a density of 1×10^6 cells/well. Cotransfections were done with CellFectin (Invitrogen) according to manufacturer's instruction at a 10:1 ratio of test plasmid to armadillo-GFP ubiquitous reporter to detect transfected cells.

Typical transfection efficiencies were about 30%. Two different control plasmids were used: empty vector and pMTAL-TAP (Tenev et al., 2002). Two days after transfection cells were split into 12 wells of 24-well plates, and some of them copper induced. Micrographs were taken at about 60 hr post treatment and then flow cytometric analysis was conducted on a FACScan machine using Cell Quest software. Stable transfection of Kc167 was performed similarly except pHygro plasmid was also used (for selection) and selected with Hygromycin.

Identification and molecular characterization of xrp1 mutant strains

J3E1. From adult homozygotes total RNA was isolated using a High Pure RNA isolation kit (Roche), and with a primer pair (5'primer- 5'GTAGTATCGATATGGCATTCTCCGTCGAAG, 3'primer- 5'AGTTCCTGCTCCTGGTTGATG) RT-PCR by using One-Step RT-PCR kit (Invitrogen) was performed. A smaller RT-PCR product was detected from the xrp1 J3E1 mutants compared to yw, this was sequenced and found to contain a 242 bp deletion which causes frameshift mutation. Genomic PCR with various primer pairs mapped the deletion to the intron between 3rd and 4th exons (please look at the Figure 2). In addition, southern blotting was performed (described below).

Xrp1 synthetic mutation. The primer pair (mentioned above) that spans the common breakpoint in both Exelixis deletions (Df(3R)Exel6181 and Df(3R)Exel6182), 5' primer at 3rd exon and 3' primer at 4th exon, was used to validate the xrp1 synthetic mutation (deletions in trans).

Southern and Northern Blotting. Southern blotting and hybridization was performed as in (Molecular Cloning). Radiolabelled probe was prepared by using DECAprime II DNA labeling kit, and for hybridization ULTRAhyb buffer (Ambion) was used. Template for probe was prepared by PCR with following primers: 5' primer- 5'GTAGTATCGATATGGCATTCTCCGTCGAAG, 3' primer- 5'TTTGGCTTGCTGTCTATCACGATCG. XhoI restriction enzyme was used for genomic DNA digestion. For Northern blotting total RNA samples were run on gels, transferred to membranes, and hybridized with ³²P-radiolabeled xrp1-specific probe (Maniatis et al., 1989; Nordstrom et al., 1996).

Immunohistochemistry. Cell cycle assay by phosphohistone H3 staining ~4 hr after ionizing radiation was performed as described previously with minor modifications (Chew et al., 2004; Ollmann et al., 2000). 3rd instar larvae were dissected in PBS-4% formaldehyde and washed with PT

(PBS with 0.1% Triton-X100) and then with PBT (PBS, 0.1% Triton-X1000, 1% BSA). PBT+NGS (PBT, 0.1% BSA, 5% normal goat serum) was used as a blocking solution. 1:200 dilution of anti-phosphohistone H3 antibody (Upstate) was incubated overnight at 4°C. The labeling was visualized with a biotinylated anti-rabbit secondary antibody and avidin-fluorescein (Vector Laboratories).

***mwh* Assay (a loss-of-heterozygosity (LOH) assay).** *mwh*¹ was recombined onto the *Xrp1* deficiencies, *Df(3R)Exel6181* or *Df(3R)Exel6182*. Animals with genotypes *mwh*¹,*Df(3R)Exel6181/+*,*Df(3R)Exel6182* and heterozygous controls (*mwh*¹,*Df(3R)Exel6181/+*, and *mwh*¹,*Df(3R)Exel6182/+*) were used for the loss-of-heterozygosity (LOH) assay which has been performed as in (Sogame et al., 2003). Briefly, wandering 3rd instar larvae were treated with ionizing radiation at the indicated doses and adult wings from at least 6 individuals were assessed for *mwh* clones in blinded counts.

Embryo Staining. Preparation of embryos, irradiation challenge, and staining for LacZ was conducted as in (Nordstrom et al., 1996). Briefly, about 0-8 hr old P1569/TM3,Sb embryos were radiation treated (40 Gray)

and 90' after they were stained for LacZ (P1569 is P{PZ}(3)02515⁰²⁵¹⁵). A SURF student, Jackie Nguyen, carried out the experiment.

Results

Ionizing radiation induces Xrp1 transcription

In an effort to identify ionizing radiation (IR) responsive genes, a screen for IR-inducible loci, was performed on enhancer trap *Drosophila* lines. In the screen about 700 lines corresponding to unique homozygous lethal insertions of P-elements containing a B-gal reporter gene were exposed to ionizing radiation. Of these, one line designated P1569, demonstrated acute induction of B-gal gene in response to ionizing radiation (Figure 4.1A). As seen in Figure 4.1A, widespread induction of the LacZ reporter is seen after ionizing radiation whereas unexposed siblings exhibit a pattern of marginal expression near the pharynx. P1569 (synonym P{PZ}l(3)02515⁰²⁵¹⁵), is a LacZ containing 'enhancer-detector' transposon inserted in the third intron of the CG17836 locus. We have named CG17836 as Xrp1 (x-ray responsive protein 1). This candidate gene, XRP1, encodes an AT-hook member of the HMG-motif proteins (Figure 4.1D). The broadly conserved AT-hook motif found in Xrp1 is shared among numerous nuclear proteins with AT-rich DNA binding activities (Aravind and Landsman, 1998). In addition, it has a nuclear localization sequence and a bZIP domain at the C-terminus (Fassler et al., 2002). Therefore, most probably Xrp1 is a nuclear protein with DNA-

binding activity. Although there is no clear mammalian homolog of Xrp1, it is highly conserved among *Drosophila* species (Figure 4.1E).

To determine the locus that is IR-responsive, northern blot analysis of wild type embryos before and after irradiation was performed. As expected it directly demonstrated the induction of XRP1 transcription by IR (Figure 4.1B). Induction of XRP1 expression upon IR treatment was also observed in cell culture. Kc cells treated with 28 kRad IR upregulate XRP1 as detected by semi-quantitative RT-PCR (Figure 4.1C). Both the northern and the Kc cell data demonstrate that regulation of XRP1 in response to the genotoxic stress occurs via transcriptional mechanisms.

An independent effort to identify IR responsive genes by microarray analysis (by other lab members) also demonstrated the robust response of XRP1. Induction level of XRP1 was the highest among IR responsive genes (not shown). Surprisingly genotoxic damage induced XRP1 expression was dmp53- dependent and it raises questions whether XRP1 is an effector of dmp53. Microarray analysis of *Drosophila* embryos by other groups also demonstrates the induction of XRP1 after genotoxic stress (IR) (Brodsky et al., 2004). Taken together our data confirm the IR response of XRP1.

Identification and molecular characterization of xrp1 mutant strains

J3E1 allele:

To understand the biological function of the corresponding gene, deletions of the XRP1 locus were produced by excising the P-element in P1569 strain through the introduction of transposase. A small percentage of excisions are imprecise. As these efforts were underway I obtained a useful deletion strain from an outside group (Mathew et al., 2002), designated J3E1 that was not precisely mapped. To characterize the deletion molecularly, I performed RT-PCR for different parts of the transcript. RT-PCR with primers 1 and 2 (Figure 4.2A) together with adult RNA detected a shorter product from the XRP1 locus in J3E1 mutants compared to yw (Figure 4.2B). The RT-PCR product was sequenced and a 242 bp deletion was identified. This deletion causes a frameshift mutation in the hypothetical ORF (colored part of 4th exon, Figure 4.2A). Furthermore, genomic PCR with various primer pairs mapped the deletion to the intron between 3rd and 4th exons (brackets, Figure 4.2D). Southern blotting was also performed to analyze the locus. Southern blotting with a probe and restriction sites (indicated by vertical arrows, Figure 4.2A) display a shorter genomic fragment in J3E1 (E1) mutants (Figure 4.2C). Together these data demonstrate that the J3E1 mutation is a deletion that removes part of the third intron and a portion of the fourth exon, indicated by the bracketed dashed line (Figure 4.2A). J3E1 homozygous flies are

much less motile than wild type, and the cultures in general are not healthy.

Synthetic allele:

Recently a new collection of precise deletion lines were released (Parks et al., 2004). Parks et al. used FLP recombinase and the large array of FRT-bearing insertions to generate deletions with molecularly defined endpoints. When I checked the collection for deletions covering *xrp1* there were two of them generated by using a transposable element inserted in *xrp1* locus (P(XP)d06938, Figure 4.3A). The two deletions, Df(3R)Exel6181 and Df(3R)Exel6182, have a common break point in an XRP1 intron and each one deletes a part of ORF. Putting these two deletion lines *in trans* generated a synthetic mutation at the *xrp1* locus. To confirm the loss of *xrp1* expression in this allele, RT-PCR analysis with adult RNA and the primer pair (see Figure 4.2A) that spans the common breakpoint in both Exelixis, 5' primer at 3rd exon and 3' primer at 4th exon, was performed. These primers detect a 1.1 kb band from wild type adults but no RT-PCR product was detected in RNA from the synthetic *xrp1* mutant, Df(3R)Exel6181 / Df(3R)Exel6182 (shown as 6181/6182). Trans-heterozygotes of J3E1 and the deletions produced only the J3E1 specific shorter fragment (Figure 4.3B). Control for the reaction, *rp49*, was indistinct for each genotype (not shown).

Animals carrying a synthetic deletion for *xrp1* were viable and fertile, and no obvious defects were observed. Because the synthetic mutant line is healthier and propagates well, the synthetic allele was used for the functional analysis of *xrp1* unless indicated otherwise.

Xrp1 promotes genomic stability after genotoxic stress

To conduct a functional characterization of Xrp1, we tested whether Xrp1 has a role in apoptosis, genomic stability or the cell cycle. To evaluate whether Xrp1 might function to maintain genomic stability, I tested *xrp1* mutants using a loss-of-heterozygosity (LOH) assay that makes use of an easily scoreable phenotype, multiple wing hair (*mwh*). The principle of the *mwh* assay is based on the loss of single wild type copy of *mwh* gene in *mwh* heterozygous animals. Loss of the normal *mwh* copy is caused by chromosomal aberrations or point mutations (Figure 4.4A, (Brodsky et al., 2000b)). In contrast to wild type wings on which there is one hair from each cell, *mwh* mutant cells or wings display multiple hairs emanating from a single cell (inset, Figure 4.4B). Therefore, *mwh* assay can be used as a measure of genomic instability in somatic tissues.

Because both *xrp1* and *mwh* loci are on 3rd chromosome, *mwh*¹ was recombined onto the *xrp1* deficiencies, Df(3R)Exel6181 or

Df(3R)Exel6182. Animals with genotypes *mwh*¹,Df(3R)Exel6181/+,Df(3R)Exel6182 and heterozygous controls (Hetero-1: *mwh*¹,Df(3R)Exel6181/+, and Hetero-2: *mwh*¹,Df(3R)Exel6182/+) were used for the LOH assays. Without irradiation LOH incidence was not observed in wild type (wt) and in the mutant animals (Figure 4.4B, 0 Gray). After treatment with 250 Rad (2.5 Gray) ionizing radiation, *xrp1* mutant adults displayed increased incidence of *mwh* cells compared to wild type or heterozygous backgrounds (Figure 4.4B). Increased dose of radiation (10 Gray) demonstrates the higher rates of LOH in *xrp1* mutant animals. Thus, Xrp1 maintains genomic stability and the mutant animals display mutator phenotype after genotoxic stress.

To determine the potential role of Xrp1 in apoptosis, I examined larval wing discs after IR exposure using acridine orange (AO) staining (Brodsky et al., 2004; Sogame et al., 2003). The *xrp1*⁻ genotype did not alter this damage-induced apoptotic response (Figure 4.5A). Likewise, the effects of Xrp1 silencing in cultured cells were similarly negative, even though the gene was responsive to radiation in this model as well (not shown, Kc cells treated with IR and ecdysone, Naoko Sogame's data). Furthermore, Xrp1 overexpression (see the next section) both in Kc cells and S2 cells did not induce apoptosis. Lastly, after IR treatment *xrp1*

mutant embryos (J3E1 allele) did not exhibit altered pattern of apoptosis compared to wild type (yw) (Figure 4.5B). Together these experiments suggest that Xrp1 functions to preserve genomic stability through activities that are distinct from apoptosis.

Xrp1 overexpression prevents cell proliferation

I next tested for a possible role of xrp1 in cell cycle arrest after genotoxic stress. Wing discs from 3rd instar larvae were radiation treated and stained for phosphohistone H3 (Brodsky et al., 2004; Sogame et al., 2003). Phosphohistone H3 antibody detects cells in mitosis, and thus it is a measure of mitotic index. It has been reported previously that dmp53 is not required for radiation-induced cell cycle arrest (Ollmann et al., 2000; Sogame et al., 2003). As shown before, 4 hr after IR treatment there are a few cells detected by the antibody in contrast to hundreds of them prior to the treatment in wt discs (Figure 4.6). Xrp1 mutant discs demonstrate the same response as wild type discs and it does not affect cell cycle arrest 4 hr after IR treatment (Figure 4.6).

To test whether Xrp1 may modify exit from the cell cycle arrest, phosphohistone staining was performed at different time points after IR treatment (as in chapter 2). Similar to dmp53 (Figure 2.7, chapter 2) loss of xrp1 did not modify the kinetics of reentry from the arrest (not shown).

Therefore, in wing discs, Xrp1 is not required for entry into cell cycle checkpoints after IR, nor does it affect exit from this arrest.

Xrp1 loss-of-function analysis demonstrates a role in genomic stability (Figure 4.4). However, in the models tested, I detected no roles in apoptosis or cell cycle arrest after genotoxic stress. To analyze its possible function when upregulated I overexpressed Xrp1 in cultured cells. Xrp1 was cloned into a metal-inducible expression vector, pMTAL-Xrp1. pMTAL-Xrp1 was cotransfected with a ubiquitiously driven GFP vector to identify Xrp1 transfected cells. After 60 hr copper (+Cu) induction of xrp1 expression, an obvious difference in GFP+ (transfected) cell numbers was observed (Figure 4.7A). Xrp1 overexpression prevented cell proliferation but the controls did not (compare top panels –Cu and +Cu). It is obvious that Xrp1 overexpression panel has much fewer doublets or triplets of cells compared to others indicating arrest of cell proliferation. The quantification of GFP+ cells show about three times less cell number in Xrp1 transfected cells after induction (Figure 4.7B). The prevention of cell proliferation was also observed in stable transfected Kc167 cells (Figure 4.7C). Thus, Xrp1 overexpression in cell culture systems prevents cell proliferation. To quantify the ratio of transfected cells to untransfected ones I conducted FACS analysis 60 hr after the induction (Figure 4.8). Overexpression of Xrp1 decreases GFP+ cells from about 30% to 12%

(Figure 4.8A). But copper induction of the control did not affect cell number (compare –Cu and +Cu panels). Quantification of multiple experiments by flow cytometry of the transfected (GFP+) cells in panel A (Figure 4.8B) confirms our microscopic analysis (Figure 4.7), and demonstrates a pronounced cytostatic effect of Xrp1 overexpression.

Discussion

Treatment of cells with DNA-damaging agents causes the transcriptional upregulation of some genes, many of which remain to be characterized (Friedberg, 2003). Our initial aim was to identify genes that are induced by IR similar to proapoptotic gene reaper (White et al., 1994). The project, functional characterization of xrp1 (CG17836), has been initiated by discovering the robust induction of xrp1 by ionizing radiation. Xrp1 expression is increased after IR in early embryos and Kc cells. The expression is also increased in larval/pupal stages by the treatment as reported in (Lee et al., 2003). Furthermore microarray data of our lab and others (Brodsky et al., 2004) reveal xrp1 as one of the top genes regarding the induction level upon IR treatment.

The Xrp1 protein appears distantly related to a UV radiation resistance associated mRNA described in the mouse (locus BC034176). There are clear homologs of it in other *Drosophila* species of which's genomes are sequenced (Figure 4.1E and Flybase). The locus encodes two isoforms, one lacks about 1/3 of the longer ORF from N-terminus. Both computational proteins have the domains discussed below. Xrp1 is reported as one of basic Zipper proteins in *Drosophila* with the domain at the very C-terminus (Fassler et al., 2002). bZIP transcription factors bind to DNA as dimers and in general require signal-induced modification to

function (Fassler et al., 2002). Xrp1 has also a very conserved motif across species called AT-hook. Some High Mobility Group (HMG) proteins have AT-hook motif through which they bind to minor groove of AT-rich genomic regions and bend DNA (Reeves and Beckerbauer, 2001; Travers, 2000). AT-hook motif is present almost exclusively in nuclear proteins (Aravind and Landsman, 1998; Bianchi and Beltrame, 2000; Reeves and Beckerbauer, 2001). In addition to bZIP and AT-hook, Xrp1 has bipartite nuclear localization sequence. The domain structure of Xrp1 indicates that Xrp1 is most likely a nuclear protein with a DNA-binding activity.

Two deletion mutations were identified and characterized. The J3E1 deletion was spuriously generated by Mathew et al when they were searching for modifiers of expression of *gukh* gene 60 kb downstream of *xrp1* locus (Mathew et al., 2002). I have mapped the deletion and found out that the deletion causes a frameshift mutation. In addition, using two Exelixis precise deletions that overlap at the *xrp1* locus in trans generated a synthetic mutant allele. Although J3E1 mutant culture is not as healthy as the synthetic mutants, they both survive to adulthood and they seem normal in gross morphology.

A potential role of Xrp1 in genomic stability was tested by a LOH assay. Without the stimulus *xrp1* mutant background did not affect LOH

rate. But IR treatment at two different doses resulted in higher rate of LOH in mutants compared to wild type animals. Thus Xrp1 maintains genomic stability after IR challenge similar to *dmp53* (Sogame et al., 2003). Initial studies with the synthetic mutant larvae exhibited much lower eclosion rate after the challenge. Because the synthetic mutants are heterozygous for so many genes including lethal ones, we do not know yet whether the lethality maps to the *xrp1* locus. Experiments are underway with the deletion controls.

To account for the instability phenotype, we reasoned that *xrp1* might function in stress-induced apoptotic responses. But the potential role of Xrp1 in apoptosis is unlikely based on following observations. First, the *Xrp1⁻* genotype did not alter wing discs cell death after IR exposure. Second, Xrp1 silencing in cultured cells did not affect cell death response to radiation/ecdysone treatment. Third, IR treatment of *xrp1* mutant embryos (*J3E1* allele) did not result in higher or lower rates of apoptosis compared to wild type. Lastly, Xrp1 overexpression both in Kc cells and S2 cells did not induce apoptosis. Therefore Xrp1 may not play a significant role, if any, in apoptosis, and so apoptosis may not account for Xrp1-mediated genomic stability.

Next I have analysed the role of Xrp1 in cell division upon the damage. IR challenge of larval wing discs results in cell cycle arrest as

assessed by the phosphohistone-staining assay. Dmp53 does not affect the arrest (Figure 2.7), however, it was still possible that Xrp1 plays a role. Xrp1⁻ background did not affect the cell cycle arrest nor did it modify dynamics of reentry to cell cycle. Nevertheless, inducible expression of Xrp1 in S2 and Kc cells prevented cell proliferation contrary to two different controls. Thus Xrp1 is not required for the IR-induced arrest but overexpression of it alone inhibits cell proliferation. It remains to be tested whether the arrest occurs at a specific cell cycle stage. The inhibition of cell proliferation might also indicate a possible explanation to the maintenance of genomic stability by Xrp1. While the precise mechanism by which this protein preserves genomic stability is not yet known, it might do it by modifying cell cycle and/or DNA repair systems.

I have noticed that Xrp1 inducible expression in cell culture dampened the GFP signal from the cotransfected reporter. As reported long time ago, ionizing radiation inhibits transcription in mammalian, yeast, insect and other cells in a dose-dependent fashion (Luchnik et al., 1988). Even though it is a total speculation right now, it is a possibility that Xrp1 might be a general transcription repressor that binds to general AT-rich promoter elements.

Expression profiling effort in the lab by others determined the radiation induced, dmp53-dependent (RIPD) 35 genes. There are two

bZIP transcription factors on the list, and as mentioned, xrp1 is one of them. The other one also is not a characterized gene, CG6272. Considering total 27 bZIP proteins in the *Drosophila* genome (Fassler et al., 2002), the likelihood of two of them in the RIPD list is very low ($\sim 10^{-5}$). Whether Xrp1 acts together with CG6272 to function remains to be tested.

Is Xrp1 an effector of dmp53? Even though xrp1 is a dmp53-dependent gene in embryos, xrp1 locus does not have dmp53-binding element and thus direct regulation of xrp1 transcription by dmp53 remains to be tested. Both dmp53 and xrp1 mutants display higher rates of LOH after IR challenge so that they maintain genomic stability (Figure 4.4 and (Sogame et al., 2003)). Also neither dmp53 nor xrp1 modify IR-induced cell cycle checkpoints. Xrp1 overexpression inhibits cell proliferation, but surprisingly overexpression of dmp53 in cells was not reported. One important difference is that dmp53 is required for IR-induced apoptosis in contrast to xrp1. Furthermore, gl-dmp53 produces rough eye phenotype (Ollmann et al., 2000) but J3E1 did not modify the gl-dmp53 'roughness' (not shown). In summary, while the precise mechanism by which this protein preserves genomic stability is not yet known, it seems likely that Xrp1 acts in p53 response pathways unrelated to cell death.

Future Directions

In development, Xrp1 expression is absent during early embryogenesis but increases dramatically at late embryogenesis and it is expressed thereafter (data is from a genome-wide expression profiling of *Drosophila* genes, (Stolc et al., 2004)). Late embryos are very resistant to IR and Xrp1 expression pattern coincides with it. Even though xrp1 mutant embryos do not modulate apoptotic response, we do not know whether the gene is responsive to IR at this stage at all. Also, to demonstrate whether Xrp1 is a general transcription repressor upon treatment we can look at several reporter systems in xrp1 mutant embryos with IR challenge and see dampening of the reporter.

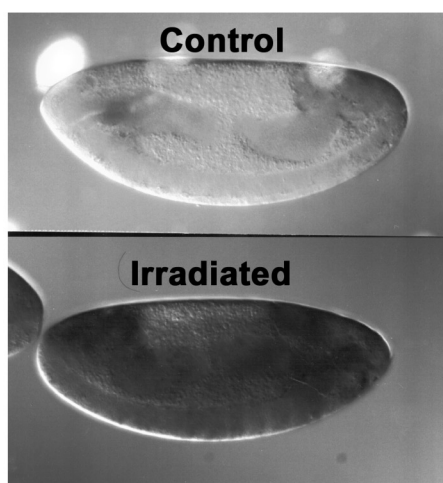
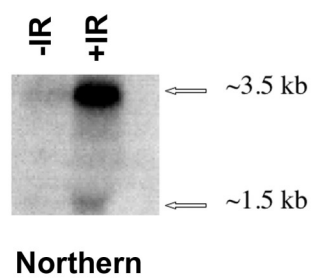
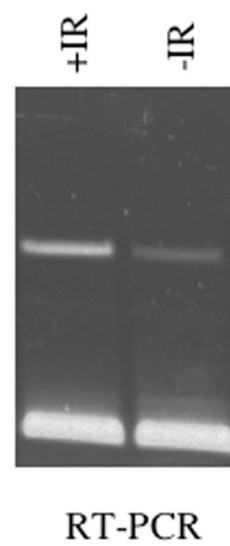
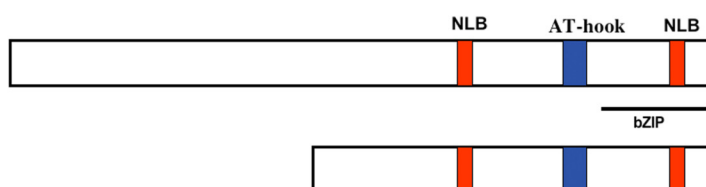
As discussed, xrp1 locus is robustly responsive to ionizing radiation. We assume that IR makes DNA strand breaks and xrp1 induction is initiated by the breaks. To directly demonstrate this and to exclude other effects of IR, the strand breaks can be induced enzymatically e.g. by Flp-FRT system, and then tested for xrp1 expression level.

We do not know whether xrp1 response is specific to IR. Do Topoisomerase inhibitors, which make strand breaks, induce it? How about alkylating agents, UV treatment or others? Answer to this will tell us whether xrp1 induction is damage specific or not and facilitate to put Xrp1

in a signaling context.

We have generated polyclonal antibody against Xrp1 and we have not yet tested it. We can use it to find out Xrp1 cellular location, and look at where Xrp1 binds in chromosomes e.g. DNA break points. It can be used also to determine binding partners by coimmunoprecipitation experiments. Furthermore, the antibody could be used as a marker to detect strand break induced signaling.

Inducible expression of Xrp1 in cell culture prevents cell proliferation. To validate this result in vivo and for other experiments we decided to generate UAS-Xrp1 transgenic animals. The vector is already generated and ready to inject. We think it will be a good resource to dissect further Xrp1 function.

A**B****C****D**

E

```

melanogaster 1 MIQEPARVQATPTATIRDNKYQTT-----AGTYSSEMS-
pseudobscura 1 MIQEPARVQATPTATIRDNKYQTT-----AGTYSSEMS-
buzzatii 1 MIQEPARVQATPTATIRDNKYQTT-----AGTYSSEMS-
willistoni 1 MIQEPARVQATPTATIRDNKYQTT-----AGTYSSEMS-

melanogaster 41 SRRTRPTPTKDSSTT-----ITIPIVIDSAPNPAILLIRVPTNRGNN
pseudobscura 59 SRRTRPTPTKDSSTT-----ITIPIVIDSAPNPAILLIRVPTNRGNN
buzzatii 38 SRRTRPTPTKDSSTT-----ITIPIVIDSAPNPAILLIRVPTNRGNN
willistoni 45 SRRTRPTPTKDSSTT-----ITIPIVIDSAPNPAILLIRVPTNRGNN

melanogaster 90 NNSTRSGTHRAFTTHIRIPFLPGSVPTAPSNQAPASSELVNPISARRCHS-
pseudobscura 103 -QAQTQTHATKCAPRTHIRIPFLPGSVPTAPSNQAPASSELVNPISARRCHS-
buzzatii 82 ---HNSNNHAKSAPRTHIRIPFLPGSVPTAPSNQAPASSELVNPISARRCHS-
willistoni 104 SSNNKNNHAKSAPRTHIRIPFLPGSVPTAPSNQAPASSELVNPISARRCHS-

melanogaster 149 -VPTTTLTSSRSP-----ETVAGLPTAMNCTVPLSAPCTTLASMAAG
pseudobscura 161 -VATSTATYQLEHSAQAPRTLHHEQATVTVTRVEMTCTVPS-TPQSOTLASHAG
buzzatii 139 IFRPLNGIYFEPSCSSASPVNVANDQDLPTFQVPTCTVPS-TPQSOTLASHAG
willistoni 163 ASSPMTIPKQSTMSHPVAIDTFGPPTATEVTEETVQVS---MQTLASHAG

melanogaster 195 IQLTGADLPSRRVVGAMPTATVEIDVVFID-----EYL
pseudobscura 219 IQLTGADLPSRRVVGAMPTATVEIDVVFID-----EYL
buzzatii 196 IQLTGADLPSRRVVGAMPTATVEIDVVFID-----EYL
willistoni 220 IQLTGADLPSRRVVGAMPTATVEIDVVFID-----EYL

melanogaster 232 QDIATSSSCNENGL---EIFTETDILDGFDINMFAEHLIELEGGTTFFSPANGM
pseudobscura 256 QDIATSSSCNENGL---EIFTETDILDGFDINMFAEHLIELEGGTTFFSPANGM
buzzatii 232 QDIATSSSCNENGL---EIFTETDILDGFDINMFAEHLIELEGGTTFFSPANGM
willistoni 280 QDIATSSSCNENGL---EIFTETDILDGFDINMFAEHLIELEGGTTFFSPANGM

melanogaster 288 NDNLDLFLNLN-----NNEETFNNSNSGVGINQEQELDFINIFHNSQPTAMT
pseudobscura 312 NDNLDLFLNLN-----NNEETFNNSNSGVGINQEQELDFINIFHNSQPTAMT
buzzatii 290 NDNLDLFLNLN-----NNEETFNNSNSGVGINQEQELDFINIFHNSQPTAMT
willistoni 338 NDNLDLFLNLN-----NNEETFNNSNSGVGINQEQELDFINIFHNSQPTAMT

melanogaster 343 SEEFYLA-YQATSTST--TFPIEPELLADMTFD--ISTTSQW-LGFLVEDVS
pseudobscura 362 GQDPMLS-FFQSTTN-----TFPIEPELLADMTFD--ISTTSQW-LGFLVEDVS
buzzatii 342 S--DFMLP-AVQVFEWSSQTRYNELIIPADENSM---NFCQQQLGFG-VGQLS
willistoni 390 NDNLDLFLNLN-----NNEETFNNSNSGVGINQEQELDFINIFHNSQPTAMT

melanogaster 397 --GSFASSEDVAATPAPQHIIITNKRSPFVPS-----PTKRKRIMLQKTELA
pseudobscura 415 PVTDPHIGGSISVAIRHTLNLNLS-LKRTASAVVAPAGETQAKRKRIMLQKTELA
buzzatii 395 --ENNDDVT--AVVHDAPTLCTV-VERTASASISVEMFQKRKRIMLQKTELA
willistoni 449 FGENIPEQENIADLQNLSSVGE---STAFKRSVLEPPTQPKRKRIMLQKTELA

melanogaster 450 PAFSP-----TPEITNLLNDDNF-----EPTTSTSTSTNTSSSTN
pseudobscura 474 PAFSP-----TPEITNLLNDDNF-----EPTTSTSTSTNTSSSTN
buzzatii 447 SQITHPVINTDIEDVYLK-----LCEINPASHISNQNQ--
willistoni 505 LLESDDVGTQIINDVLSSTTENDTLKYQFYQNINRFYQPNVEDDRPTPNAETN

melanogaster 491 ADIVDLRSAAEETTT---DFSAPNTFHNYSASS-CAAPTCQYGGFLTAPASPAY
pseudobscura 533 ADIVDLRSAAEETTT---DFSAPNTFHNYSASS-CAAPTCQYGGFLTAPASPAY
buzzatii 482 --YHELRSAAEETTT---DFSAPNTFHNYSASS-CAAPTCQYGGFLTAPASPAY
willistoni 565 DKIVDLRSAAEETTT---DFSAPNTFHNYSASS-CAAPTCQYGGFLTAPASPAY

melanogaster 546 STASTVFPSPACLS-KKRGKRPANADGGDFVLSNKSSEERKAYQRLNNEA
pseudobscura 588 STASTVFPSPACLS-KKRGKRPANADGGDFVLSNKSSEERKAYQRLNNEA
buzzatii 540 STASTVFPSPACLS-KKRGKRPANADGGDFVLSNKSSEERKAYQRLNNEA
willistoni 618 STASTVFPSPACLS-KKRGKRPANADGGDFVLSNKSSEERKAYQRLNNEA

melanogaster 605 SVSRRAKTVPLEEKRAEDTLAENLRARADEASRKRKTKYLNENQKSTYVQ
pseudobscura 647 SVSRRAKTVPLEEKRAEDTLAENLRARADEASRKRKTKYLNENQKSTYVQ
buzzatii 598 SVSRRAKTVPLEEKRAEDTLAENLRARADEASRKRKTKYLNENQKSTYVQ
willistoni 647 SVSRRAKTVPLEEKRAEDTLAENLRARADEASRKRKTKYLNENQKSTYVQ

melanogaster 665 QD-
pseudobscura 707 E---
buzzatii 658 SPAS
willistoni ----

```

Figure 4.1. Stress induction of Xrp1 occurs by transcription. (A) P1569 is an 'enhancer trap' strain inserted at the *xrp1* locus which detects ionizing radiation (IR)-responsive activity (see Figure 4.3A). Shown here are P1569 embryos stained for LacZ activity 90' after challenge by IR (4 kRad), or after mock treatment (Control). (B) *xrp1* encodes ionizing radiation inducible transcripts. Equal amounts of RNA from control (-IR) and irradiated embryos (+IR) were probed with an *xrp1* specific probe. Irradiated RNA was prepared from early staged embryos 90 minutes after exposure to 4000 rads. Large mRNA is ~3.5kb, small mRNA is ~1.5kb. (C) Similarly Kc cells were treated with 28 kRad IR and RT-PCR was performed with a primer pair (see Materials-J3E1 characterization). Note to the induction of *xrp1* transcript upon IR. Lower band is a control, rp49. (D) Schematized domain structure of Xrp1 isoforms. NLBs are nuclear localization sequences. AT-hook is a domain that binds AT-rich genomic DNA, and bZIP is a basic leucine zipper domain. (E) Multiple alignments of Xrp1 homologs of *Drosophila* species. Xrp1 homologs were identified by BLAST analysis, and CLUSTAL-W was used to generate the alignment. Notice to the highly conserved regions throughout the protein. (Contributions: SURF student, Jackie Nguyen, carried out the screen. W.F. Nordstrom generated the Northern data)

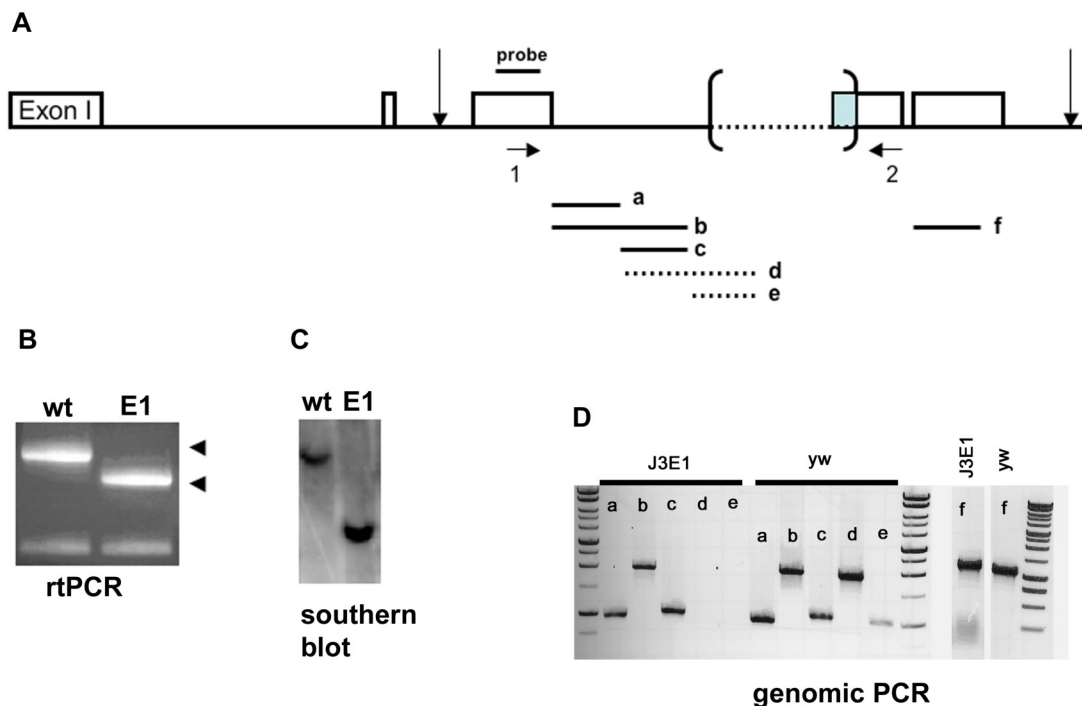


Figure 4.2. Identification and molecular characterization of the *xrp1* locus. **(A)** Schematized genomic structure of the *xrp1* locus. Included are exons (rectangles) and relevant primers. **(B)** An uncharacterized deletion strain at the *xrp1* locus, J3E1 (shown as E1), was generated by the mobilization of J3 insertion in the intron between 3rd and 4th exons by Mathew et al, and characterized here using RT-PCR (B) and southern blotting (C). RT-PCR with primers 1 and 2 (panel A) detected a shorter product from the *xrp1* J3E1 mutants compared to yw (arrow heads) from adult homozygote total RNA. Lower band is a control with rp49 specific primers. The RT-PCR product was sequenced and 242 bp deletion was identified which causes frameshift mutation (colored part of 4th exon, panel A). **(C)** Southern blotting with a probe and restriction sites (indicated by vertical arrows, panel A) display a shorter genomic fragment in J3E1 (E1) mutants. **(D)** Genomic PCR around the J3E1 deletion. Genomic PCR with various primer pairs mapped the deletion to the intron between 3rd and 4th exons (brackets and dashed line). PCR products are labeled by the letters, which correspond to genomic regions as labeled in panel A. Note that f fragments were examined on a separate gel.

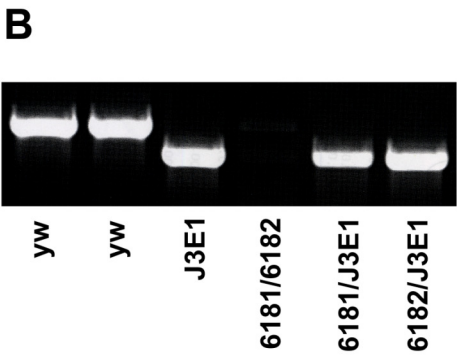
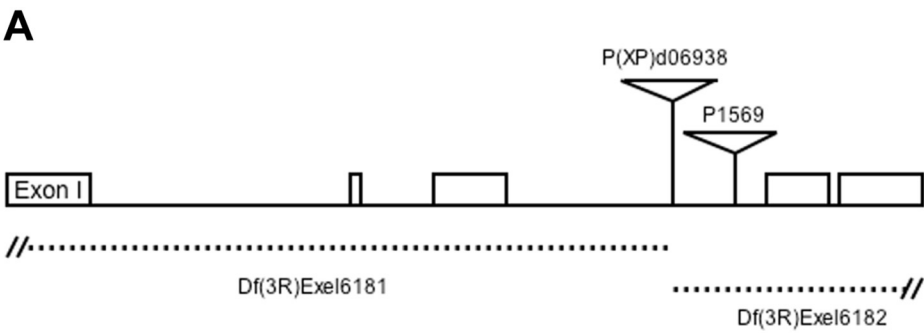


Figure 4.3. Xrp1 synthetic mutation. (A) Displayed are the relevant P-element strains and deletions (dashed lines) used to produce a synthetic mutation at Xrp1. The P-element, P(XP)d06938, was used to derive deletion strains Df(3R)Exel6181 and Df(3R)Exel6182 (Parks et al., 2004). P1569 is an unrelated transposon insertion in the 3rd intron detected in the screen and depicted in Figure 4.1. **(B)** Lack of Xrp1 expression was confirmed in animals trans-heterozygous for Df(3R)Exel6181/Df(3R)Exel6182. The primer pair (see Figure 4.2A) that spans the common breakpoint in both Exelixis deletions (Df(3R)Exel6181 and Df(3R)Exel6182), 5' primer at 3rd exon and 3' primer at 4th exon, was used to validate the xrp1 synthetic mutation (deletions in trans). These primers detect a 1.1 kb band from wild type adult RNA but no RT-PCR product was detected in RNA prepared from the synthetic xrp1 mutant, Df(3R)Exel6181 / Df(3R)Exel6182. As expected trans-heterozygotes of J3E1 and each of the deletions produced only the J3E1 specific shorter fragment.

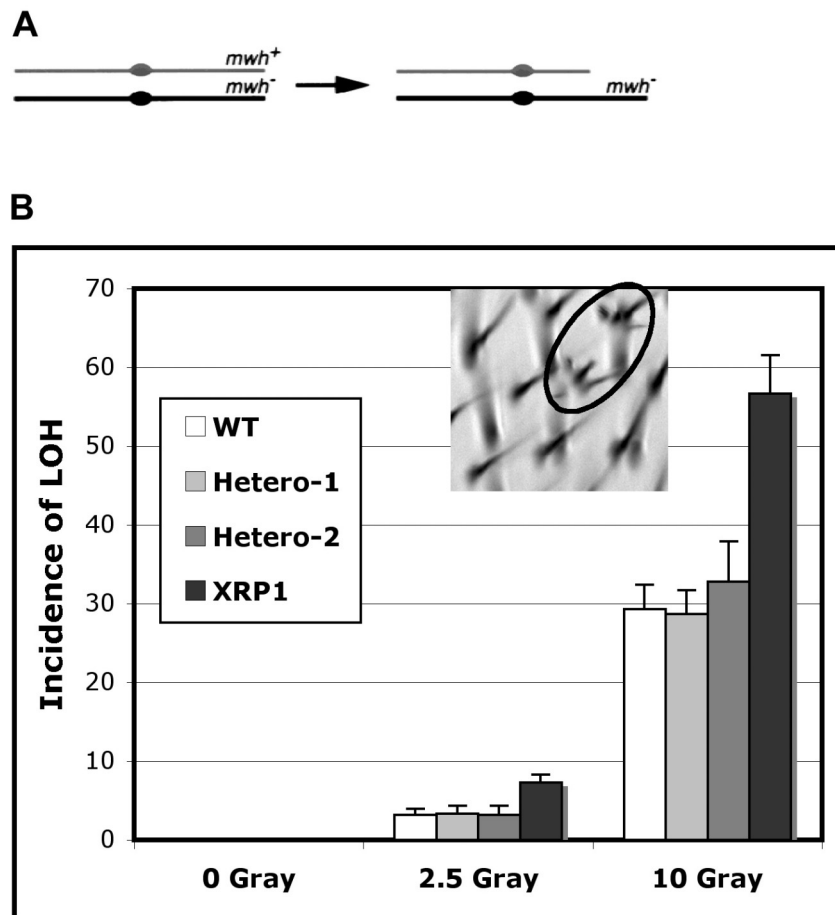


Figure 4.4. Xrp1 promotes genomic stability after genotoxic stress. (A) Principle of the multiple wing hair (*mwh*) assay (Brodsky et al., 2000b) to detect LOH (loss-of-heterozygosity). (B) Increased LOH rates in Xrp1 mutants after exposure to ionizing radiation (IR). LOH, a measure for mutant load in somatic cells, is assessed by scoring the multiple wing hair (*mwh*) phenotype in flies wild type (wt) or mutant for Xrp1 and heterozygous for *mwh*¹. Compared to wt, Xrp1 mutants display increased LOH rates after IR challenge. Inset illustrates the recessive *mwh* phenotype (circled wing hairs). Error bars, SD.

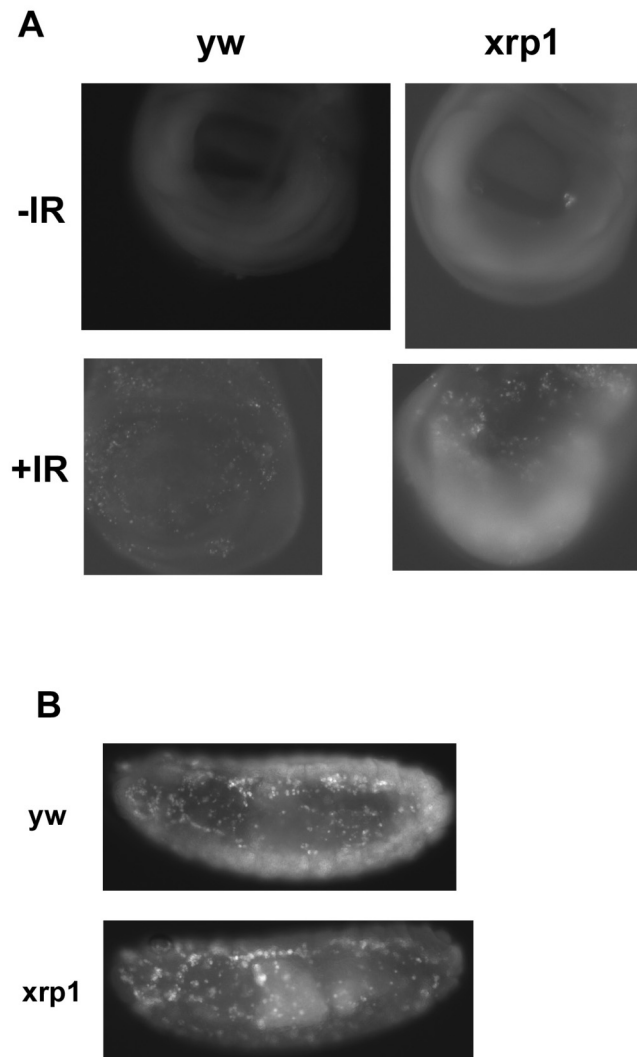


Figure 4.5. *xrp1* (J3E1 strain) is not required for ionizing radiation (IR)-induced apoptosis. (A) 3rd instar larvae were mock treated (IR-, top panels) or irradiated (IR+, bottom panels) with 40Gy. About 4 hr after irradiation apoptotic cells in wing discs were detected by using a vital dye, acridine orange (AO). *xrp1* mutation does not modulate the damage-induced apoptosis in this tissue. (B) *xrp1* does not affect embryonic cell death (PCD). *yw* and *xrp1* (J3E1) embryos were radiation treated (40Gy) and 2hrs later stained with AO to detect apoptosis. Comparably staged embryos display similar pattern and number of cell death.

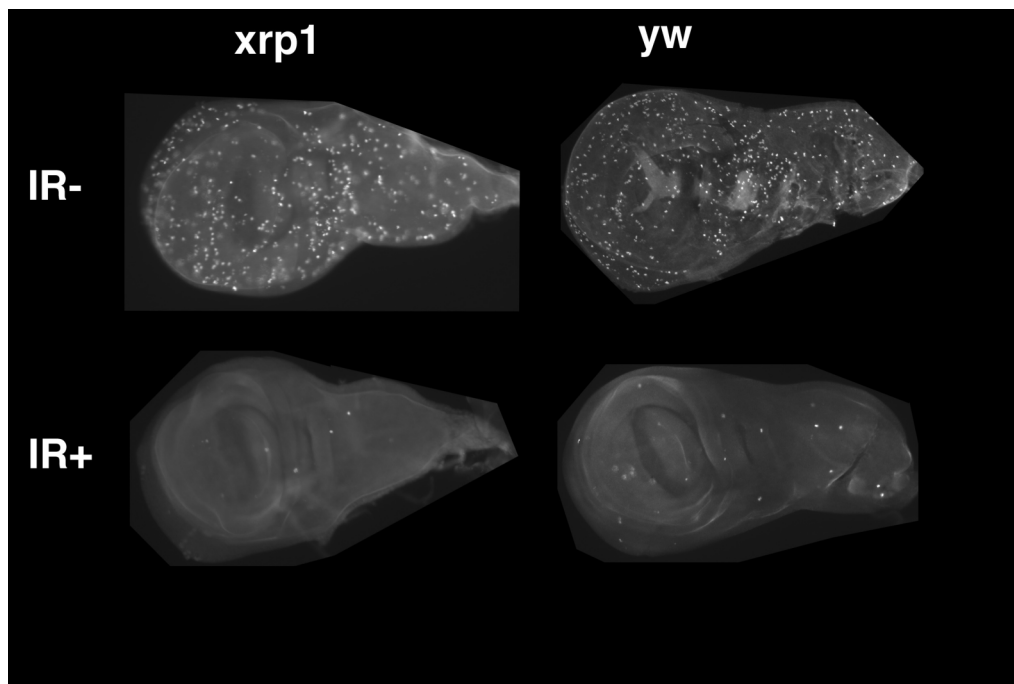


Figure 4.6. Cell cycle arrest after ionizing is unaffected by loss of *xrp1*. anti-phospho-Histone H3 antibody is used here to detect cells undergoing mitosis in the 3rd instar larval wing discs. Both wild-type (*yw*) and *xrp1* (synthetic) mutant wing discs display similar number of cells undergoing mitosis without IR treatment (top panels). To test the potential effect of *xrp1* the larvae were radiation treated (4kRad (40Gray)), wing discs were dissected and then stained about 4 hr later (bottom panels). The mitotic index of wt and *xrp1*⁻ discs were comparable at this time point and later post IR time points as well (data not shown and see Chapter-2 staining). At least 12 wing discs were examined.

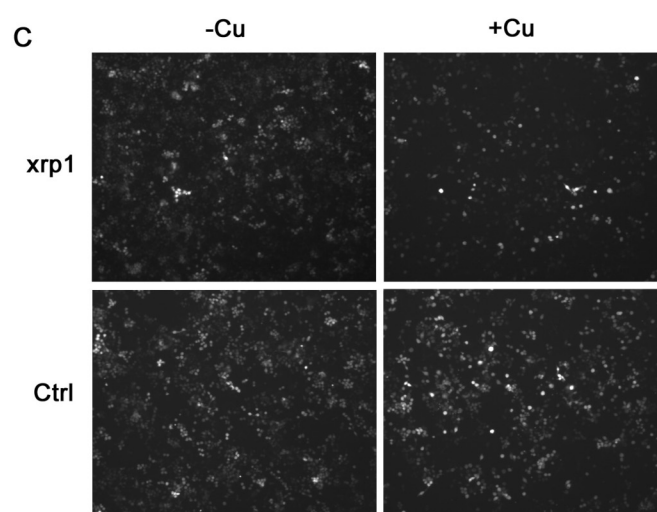
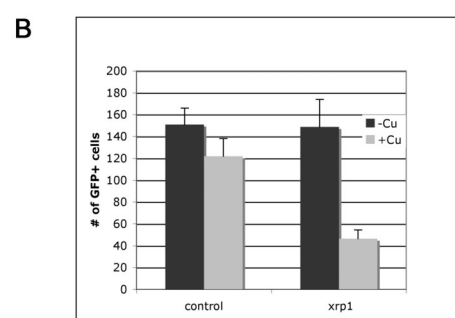
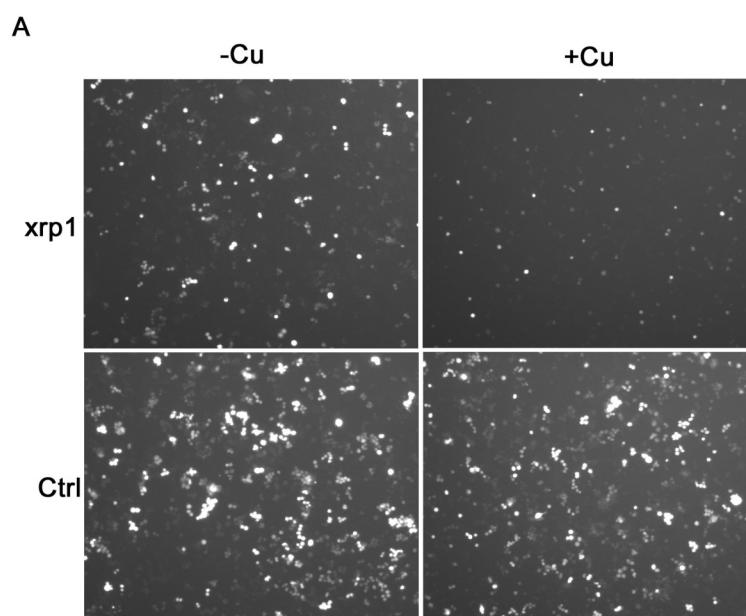


Figure 4.7. Xrp1 overexpression prevents cell proliferation. (A) S2 cells were cotransfected with a ubiquitously expressed GFP vector (arm-GFP) and pMTAL-Xrp1 (A, top panels) or with control (pMTAL-TAP) (A, bottom panels). 60 hrs after copper induction (+Cu) pictures were taken. Upon induction, bottom panels, Xrp1 display a significant block to cell proliferation (compare top panels –Cu and +Cu) not seen in the controls. Note that induction of Xrp1 prevents the appearance of doublets or triplets of GFP+ cells compared to controls. Transfection efficiencies were about 30%. (B) Counts of transfected (GFP+) cells in panel A (four independent trials and four fields from each). About 60 hrs later Xrp1 overexpression dramatically reduced cell number. Error bars, SD. (C) Xrp1 expression in stable-transfected Kc167 cells inhibits cell proliferation. Kc167 cells were cotransfected with ubiquitous GFP (arm-GFP), pHygro (for selection), and pMTAL-Xrp1 or with control (pMTAL-TAP). 3 days after copper induction (+Cu) pictures were taken. Upon induction Xrp1 prevents cell proliferation but the control does not.

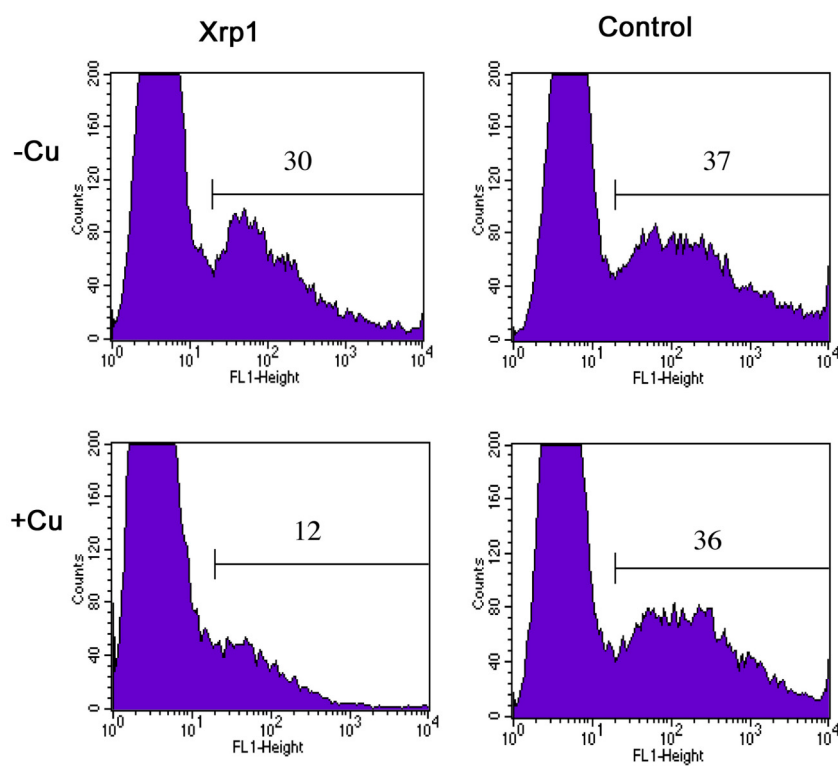
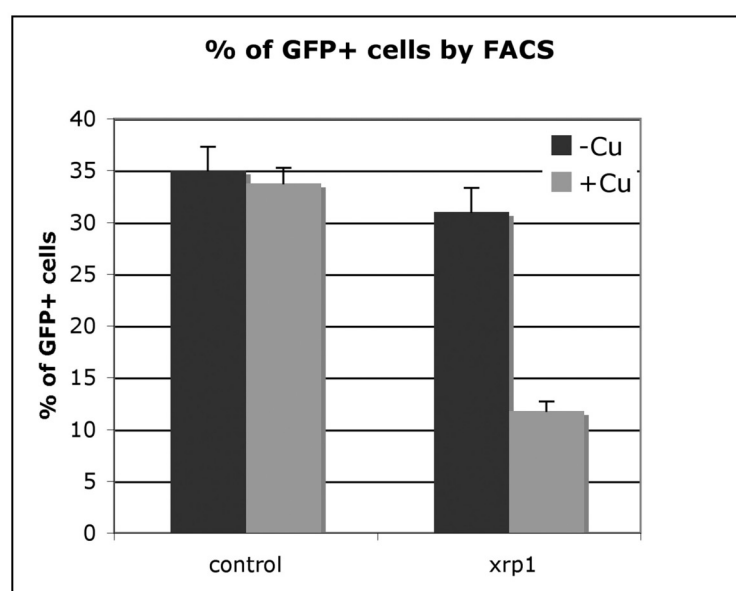
A**B**

Figure 4.8. Analysis of Xrp1-mediated proliferation arrest by flow cytometry. S2 cells were cotransfected with ubiquitous GFP (arm-GFP) and pMTAL-Xrp1 or with a control (pMTAL-TAP) as in Figure 8. 60 hrs after copper induction (+Cu) flow cytometric analysis was performed. X-axis (FL1) indicates GFP signal intensity. Notice that copper induced overexpression of Xrp1 decreases GFP+ cells from about 30% to 12%. But copper induction of the control does not affect the incidence of these cells (compare –Cu and +Cu panels). (B) Quantification of multiple experiments by flow cytometry of the transfected (GFP+) cells in panel A. Error bars, SD.

Bibliography

Abrams, J. M. (1999). An emerging blueprint for apoptosis in *Drosophila*. Trends in Cell Biology 9, 435-440.

Abrams, J. M., White, K., Fessler, L., and Steller, H. (1993). Programmed cell death during *Drosophila* embryogenesis. Development 117, 29-44.

Adrain, C., Slee, E. A., Harte, M. T., and Martin, S. J. (1999). Regulation of apoptotic protease activating factor-1 oligomerization and apoptosis by the WD-40 repeat region. Journal of Biological Chemistry 274, 20855-20860.

Akdemir, F., Farkas, R., Chen, P., Juhasz, G., Medved'ova, L., Sass, M., Wang, L., Wang, X., Chittaranjan, S., Gorski, S. M., *et al.* (2006). Autophagy occurs upstream or parallel to the apoptosome during histolytic cell death. Development 133, 1457-1465.

Aravind, L., and Landsman, D. (1998). AT-hook motifs identified in a wide variety of DNA-binding proteins. Nucleic Acids Res 26, 4413-4421.

Bianchi, M. E., and Beltrame, M. (2000). Upwardly mobile proteins. Workshop: the role of HMG proteins in chromatin structure, gene expression and neoplasia. EMBO Rep 1, 109-114.

Brodsky, M. H., Nordstrom, W., Tsang, G., Kwan, E., Rubin, G. M., and Abrams, J. M. (2000a). *Drosophila* p53 binds a damage response element at the reaper locus. *Cell* *101*, 103-113.

Brodsky, M. H., Sekelsky, J. J., Tsang, G., Hawley, R. S., and Rubin, G. M. (2000b). *mus304* encodes a novel DNA damage checkpoint protein required during *Drosophila* development. *Genes & Development* *14*, 666-678.

Brodsky, M. H., Sekelsky, J. J., Tsang, G., Hawley, R. S., and Rubin, G. M. (2000c). *mus304* encodes a novel DNA damage checkpoint protein required during *Drosophila* development. *Genes Dev* *in press*.

Brodsky, M. H., Weinert, B. T., Tsang, G., Rong, Y. S., McGinnis, N. M., Golic, K. G., Rio, D. C., and Rubin, G. M. (2004). *Drosophila melanogaster* MNK/Chk2 and p53 regulate multiple DNA repair and apoptotic pathways following DNA damage. *Mol Cell Biol* *24*, 1219-1231.

Chai, J., Yan, N., Huh, J. R., Wu, J. W., Li, W., Hay, B. A., and Shi, Y. (2003). Molecular mechanism of Reaper-Grim-Hid-mediated suppression of DIAP1-dependent Dronc ubiquitination. *Nat Struct Biol* *10*, 892-898.

Chen, P., Nordstrom, W., Gish, B., and Abrams, J. M. (1996). Grim, a novel cell death gene in *drosophila*. *Genes & Development* *10*, 1773-1782.

Chen, P., Rodriguez, A., Erskine, R., Thach, T., and Abrams, J. M. (1998). Dredd, a Novel Effector of the Apoptosis Activators Reaper, Grim, and Hid in *Drosophila*. *Developmental Biology* 201, 202-216.

Chew, S. K., Akdemir, F., Chen, P., Lu, W. J., Mills, K., Daish, T., Kumar, S., Rodriguez, A., and Abrams, J. M. (2004). The apical caspase dronc governs programmed and unprogrammed cell death in *Drosophila*. *Dev Cell* 7, 897-907.

Chou, T. B., and Perrimon, N. (1996). The autosomal FLP-DFS technique for generating germline mosaics in *Drosophila melanogaster*. *Genetics* 144, 1673-1679.

Christich, A., Kauppila, S., Chen, P., Sogame, N., Ho, S. I., and Abrams, J. M. (2002). The Damage-Responsive *Drosophila* Gene sickle Encodes a Novel IAP Binding Protein Similar to but Distinct from reaper, grim, and hid. *Curr Biol* 12, 137-140.

Coates, P. J., Lorimore, S. A., and Wright, E. G. (2004). Damaging and protective cell signalling in the untargeted effects of ionizing radiation. *Mutat Res* 568, 5-20.

Danial, N. N., and Korsmeyer, S. J. (2004). Cell death: critical control points. *Cell* 116, 205-219.

Deveraux, Q. L., Takahashi, R., Salvesen, G. S., and Reed, J. C. (1997). X-linked iap is a direct inhibitor of cell-death proteases. *Nature* 388, 300-304.

Ditzel, M., Wilson, R., Tenev, T., Zachariou, A., Paul, A., Deas, E., and Meier, P. (2003). Degradation of DIAP1 by the N-end rule pathway is essential for regulating apoptosis. *Nat Cell Biol* 5, 467-473.

Dorstyn, L., Colussi, P. A., Quinn, L. M., Richardson, H., and Kumar, S. (1999). DRONC, an ecdysone-inducible *Drosophila* caspase. *Proceedings of the National Academy of Sciences of the United States of America* 96, 4307-4312.

Dorstyn, L., Mills, K., Lazebnik, Y., and Kumar, S. (2004). The two cytochrome c species, DC3 and DC4, are not required for caspase activation and apoptosis in *Drosophila* cells. *J Cell Biol* 167, 405-410.

Dorstyn, L., Read, S., Cakouros, D., Huh, J. R., Hay, B. A., and Kumar, S. (2002). The role of cytochrome c in caspase activation in *Drosophila melanogaster* cells. *J Cell Biol* 156, 1089-1098.

Drapeau, M. D., Radovic, A., Wittkopp, P. J., and Long, A. D. (2003). A gene necessary for normal male courtship, yellow, acts downstream of fruitless in the *Drosophila melanogaster* larval brain. *J Neurobiol* 55, 53-72.

Du, C. Y., Fang, M., Li, Y. C., Li, L., and Wang, X. D. (2000). Smac, a mitochondrial protein that promotes cytochrome c-dependent caspase activation by eliminating IAP inhibition. *Cell* 102, 33-42.

Ellis, H. M., and Horvitz, H. R. (1986). Genetic control of programmed cell death in the nematode *C. elegans*. *Cell* 44, 817-829.

Fassler, J., Landsman, D., Acharya, A., Moll, J. R., Bonovich, M., and Vinson, C. (2002). B-ZIP proteins encoded by the *Drosophila* genome: evaluation of potential dimerization partners. *Genome Res* 12, 1190-1200.

Friedberg, E. C. (2003). DNA damage and repair. *Nature* 421, 436-440.

Geisbrecht, E. R., and Montell, D. J. (2004). A role for *Drosophila* IAP1-mediated caspase inhibition in Rac-dependent cell migration. *Cell* 118, 111-125.

Goldstein, L. S. B., and Fyrberg, E. A. (1994). *Drosophila melanogaster*: Practical Uses in Cell and Molecular Biology, Vol 44 (San Diego: Academic Press, Inc.).

Goyal, L. (2001). Cell death inhibition: Keeping caspases in check. *Cell* 104, 805-808.

Grether, M. E., Abrams, J. M., Agapite, J., White, K., and Steller, H. (1995). The *head involution defective* gene of *Drosophila melanogaster* functions in programmed cell death. *Genes & Development* 9, 1694-1708.

Gross, A., McDonnell, J. M., and Korsmeyer, S. J. (1999). BCL-2 family members and the mitochondria in apoptosis. *Genes & Development* 13, 1899-1911.

Gudkov, A. V., and Komarova, E. A. (2003). The role of p53 in determining sensitivity to radiotherapy. *Nat Rev Cancer* 3, 117-129.

Hanahan, D., and Weinberg, R. A. (2000). The hallmarks of cancer. *Cell* 100, 57-70.

Hawkins, C. J., Yoo, S. J., Peterson, E. P., Wang, S. L., Vernooy, S. Y., and Hay, B. A. (2000). The *Drosophila* caspase DRONC cleaves following glutamate or aspartate and is regulated by DIAP1, HID, and GRIM. *J Biol Chem* 275, 27084-27093.

Hays, R., Wickline, L., and Cagan, R. (2002). Morgue mediates apoptosis in the *Drosophila melanogaster* retina by promoting degradation of DIAP1. *Nat Cell Biol* 4, 425-431.

Hu, Y. M., Ding, L. Y., Spencer, D. M., and Nunez, G. (1998). WD-40 repeat region regulates Apaf-1 self-association and procaspase-9 activation. *Journal of Biological Chemistry* 273, 33489-33494.

Huh, J. R., Guo, M., and Hay, B. A. (2004a). Compensatory Proliferation Induced Cell Death in the *Drosophila* Wing Disc Requires Activity of the Apical Cell Death Caspase Dronc in a Nonapoptotic Role. *Current Biology Online, June 3rd, 2004*.

Huh, J. R., Vernoooy, S. Y., Yu, H., Yan, N., Shi, Y., Guo, M., and Hay, B. A. (2004b). Multiple apoptotic caspase cascades are required in nonapoptotic roles for *Drosophila* spermatid individualization. *PLoS Biol* 2, E15.

Kanuka, H., Sawamoto, K., Inohara, N., Matsuno, K., Okano, H., and Miura, M. (1999). Control of the cell death pathway by Dapaf-1, a *Drosophila* Apaf-1/CED-4-related caspase activator. *Molecular Cell* 4, 757-769.

Kastan, M. B., and Bartek, J. (2004). Cell-cycle checkpoints and cancer. *Nature* 432, 316-323.

Kerr, J. F. R., Wyllie, A. H., and Currie, A. R. (1972). Apoptosis: a basic biological phenomenon with wide ranging implications in tissue kinetics. *Br J Cancer* 26, 239-257.

Kimura, K., Kodama, A., Hayasaka, Y., and Ohta, T. (2004). Activation of the cAMP/PKA signaling pathway is required for post-ecdysial cell death in wing epidermal cells of *Drosophila melanogaster*. *Development* 131, 1597-1606.

Kumar, S., and Dumanis, J. (2000). The fly caspases. *Cell Death & Differentiation* 7, 1039-1044.

Laundrie, B., Peterson, J. S., Baum, J. S., Chang, J. C., Fileppo, D., Thompson, S. R., and McCall, K. (2003). Germline cell death is inhibited

by P-element insertions disrupting the *dcp-1/pita* nested gene pair in *Drosophila*. *Genetics* **165**, 1881-1888.

Lee, C. Y., Clough, E. A., Yellon, P., Teslovich, T. M., Stephan, D. A., and Baehrecke, E. H. (2003). Genome-wide analyses of steroid- and radiation-triggered programmed cell death in *Drosophila*. *Curr Biol* **13**, 350-357.

Leulier, F., Rodriguez, A., Khush, R. S., Abrams, J. M., and Lemaitre, B. (2000). The *Drosophila* caspase Dredd is required to resist Gram-negative bacterial infection. *EMBO Reports* **1**, 353-358.

Li, L., Thomas, R. M., Suzuki, H., De Brabander, J. K., Wang, X., and Harran, P. G. (2004). A small molecule Smac mimic potentiates TRAIL- and TNF α -mediated cell death. *Science* **305**, 1471-1474.

Li, P., Nijhawan, D., Budihardjo, I., Srinivasula, S. M., Ahmad, M., Alnemri, E. S., and Wang, X. D. (1997). Cytochrome c and datp-dependent formation of apaf-1/caspase-9 complex initiates an apoptotic protease cascade. *Cell* **91**, 479-489.

Lindsten, T., and Thompson, C. B. (2006). Cell death in the absence of Bax and Bak. *Cell Death Differ*.

Liu, X. S., Kim, C. N., Yang, J., Jemmerson, R., and Wang, X. D. (1996). Induction of apoptotic program in cell-free extracts - requirement for datp and cytochrome c. *Cell* **86**, 147-157.

Luchnik, A. N., Hisamutdinov, T. A., and Georgiev, G. P. (1988). Inhibition of transcription in eukaryotic cells by X-irradiation: relation to the loss of topological constraint in closed DNA loops. *Nuc Acids Res* 16, 5175-5190.

Maniatis, T., Sambrook, J., and Fritsch, E. F. (1989). *Molecular Cloning: A Laboratory Manual*. Second Edition (Cold Spring Harbor: Cold Spring Harbor Laboratory Press).

Manseau, L., Baradaran, A., Brower, D., Budhu, A., Elefant, F., Phan, H., Philp, A. V., Yang, M., Glover, D., Kaiser, K., *et al.* (1997). GAL4 enhancer traps expressed in the embryo, larval brain, imaginal discs, and ovary of *Drosophila*. *Dev Dyn* 209, 310-322.

Martin, S. J. (2002). Destabilizing Influences in Apoptosis. Sowing the Seeds of IAP Destruction. *Cell* 109, 793-796.

Mathew, D., Gramates, L. S., Packard, M., Thomas, U., Bilder, D., Perrimon, N., Gorczyca, M., and Budnik, V. (2002). Recruitment of scribble to the synaptic scaffolding complex requires GUK-holder, a novel DLG binding protein. *Curr Biol* 12, 531-539.

Meier, P., Silke, J., Leivers, S. J., and Evan, G. I. (2000a). The *Drosophila* caspase DRONC is regulated by DIAP1. *EMBO Journal* 19, 598-611.

Meier, P., Silke, J., Leivers, S. J., and Evan, G. I. (2000b). The *Drosophila* caspase DRONC is regulated by DIAP1. *Embo J* 19, 598-611.

Mills, K., Daish, T., and Kumar, S. (2005). The function of the *Drosophila* caspase DRONC in cell death and development. *Cell Cycle* 4, 744-746.

Moriishi, K., Huang, D. C. S., Cory, S., and Adams, J. M. (1999). Bcl-2 family members do not inhibit apoptosis by binding the caspase activator Apaf-1. *Proceedings of the National Academy of Sciences of the United States of America* 96, 9683-9688.

Nakano, K., and Vousden, K. H. (2001). PUMA, a novel proapoptotic gene, is induced by p53. *Molecular Cell* 7, 683-694.

Nordstrom, W., Chen, P., Steller, H., and Abrams, J. M. (1996). Activation of the reaper gene during ectopic cell killing in *drosophila*. *Developmental Biology* 180, 213-226.

Oda, E., Ohki, R., Murasawa, H., Nemoto, J., Shibue, T., Yamashita, T., Tokino, T., Taniguchi, T., and Tanaka, N. (2000). Noxa, a BH3-only member of the Bcl-2 family and candidate mediator of p53-induced apoptosis. *Science* 288, 1053-1058.

Ollmann, M., Young, L. M., Di Como, C. J., Karim, F., Belvin, M., Robertson, S., Whittaker, K., Demsky, M., Fisher, W. W., Buchman, A., *et al.* (2000). *Drosophila* p53 is a structural and functional homolog of the tumor suppressor p53. *Cell* 101, 91-101.

Parks, A. L., Cook, K. R., Belvin, M., Dompe, N. A., Fawcett, R., Huppert, K., Tan, L. R., Winter, C. G., Bogart, K. P., Deal, J. E., *et al.* (2004).

Systematic generation of high-resolution deletion coverage of the *Drosophila melanogaster* genome. *Nat Genet* 36, 288-292.

Peters, M., DeLuca, C., Hirao, A., Stambolic, V., Potter, J., Zhou, L., Liepa, J., Snow, B., Arya, S., Wong, J., *et al.* (2002). Chk2 regulates irradiation-induced, p53-mediated apoptosis in *Drosophila*. *Proc Natl Acad Sci U S A* 99, 11305-11310.

Quinn, L. M., Dorstyn, L., Mills, K., Colussi, P. A., Chen, P., Coombe, M., Abrams, J., Kumar, S., and Richardson, H. (2000). An essential role for the caspase *dronc* in developmentally programmed cell death in *Drosophila*. *Journal of Biological Chemistry* 275, 40416-40424.

Reeves, R., and Beckerbauer, L. (2001). HMG1/Y proteins: flexible regulators of transcription and chromatin structure. *Biochim Biophys Acta* 1519, 13-29.

Rodriguez, A., Oliver, H., Zou, H., Chen, P., Wang, X. D., and Abrams, J. M. (1999). Dark is a *Drosophila* homologue of Apaf-1/CED-4 and functions in an evolutionarily conserved death pathway. *Nature Cell Biology* 1, 272-279.

Rong, Y. S., Titen, S. W., Xie, H. B., Golic, M. M., Bastiani, M., Bandyopadhyay, P., Olivera, B. M., Brodsky, M., Rubin, G. M., and Golic, K. G. (2002). Targeted mutagenesis by homologous recombination in *D. melanogaster*. *Genes Dev* 16, 1568-1581.

Ryoo, H. D., Bergmann, A., Gonen, H., Ciechanover, A., and Steller, H. (2002). Regulation of *Drosophila* IAP1 degradation and apoptosis by reaper and ubcD1. *Nat Cell Biol* 4, 432-438.

Ryoo, H. D., Gorenc, T., and Steller, H. (2004). Apoptotic cells can induce compensatory cell proliferation through the JNK and the Wingless signaling pathways. *Dev Cell* 7, 491-501.

Salvesen, G. S., and Abrams, J. M. (2004). Caspase activation - stepping on the gas or releasing the brakes? Lessons from humans and flies. *Oncogene* 23, 2774-2784.

Salvesen, G. S., and Duckett, C. S. (2002). IAP proteins: blocking the road to death's door. *Nat Rev Mol Cell Biol* 3, 401-410.

Scaffidi, P., Misteli, T., and Bianchi, M. E. (2002). Release of chromatin protein HMGB1 by necrotic cells triggers inflammation. *Nature* 418, 191-195.

Shi, Y. (2002). Mechanisms of Caspase Activation and Inhibition during Apoptosis. *Mol Cell* 9, 459-470.

Silke, J. H., Kratina, T., Ekert, P. G., Pakusch, M., and Vaux, D. L. (2003). Unlike Diablo/smac, grim promotes global ubiquitination and specific degradation of XIAP and neither cause apoptosis. *J Biol Chem*.

Sogame, N., and Abrams, J. (2003). Radiation Responses in *Drosophila*, In Handbook of Cell Signaling, R. A. Bradshaw, and E. A. Dennis, eds. (Elsevier), pp. Chapter 303.

Sogame, N., Kim, M., and Abrams, J. M. (2003). *Drosophila* p53 preserves genomic stability by regulating cell death. *Proc Natl Acad Sci U S A* 100, 4696-4701.

Spierings, D., McStay, G., Saleh, M., Bender, C., Chipuk, J., Maurer, U., and Green, D. R. (2005). Connected to death: the (unexpurgated) mitochondrial pathway of apoptosis. *Science* 310, 66-67.

Stolc, V., Gauhar, Z., Mason, C., Halasz, G., van Batenburg, M. F., Rifkin, S. A., Hua, S., Herreman, T., Tongprasit, W., Barbano, P. E., *et al.* (2004). A gene expression map for the euchromatic genome of *Drosophila melanogaster*. *Science* 306, 655-660.

Stowers, R. S., and Schwarz, T. L. (1999). A genetic method for generating *Drosophila* eyes composed exclusively of mitotic clones of a single genotype. *Genetics* 152, 1631-1639.

Tenev, T., Zachariou, A., Wilson, R., Paul, A., and Meier, P. (2002). Jafrac2 is an IAP antagonist that promotes cell death by liberating Dronc from DIAP1. *Embo J* 21, 5118-5129.

Travers, A. (2000). Recognition of distorted DNA structures by HMG domains. *Curr Opin Struct Biol* 10, 102-109.

Vaux, D. L., Cory, S., and Adams, J. M. (1988). Bcl-2 gene promotes haematopoietic cell survival and cooperates with c-myc to immortalize pre-B cells. *Nature* 335, 440-442.

Vaux, D. L., Weissman, I. L., and Kim, S. K. (1992). Prevention of programmed cell death in *Ceanorhabditis elegans* by human bcl-2. *Science* 258, 1955-1957.

Vegh, M., and Basler, K. (2003). A genetic screen for hedgehog targets involved in the maintenance of the *Drosophila* anteroposterior compartment boundary. *Genetics* 163, 1427-1438.

Wang, S. L., Hawkins, C. J., Yoo, S. J., Muller, H. A. J., and Hay, B. A. (1999). The *Drosophila* caspase inhibitor DIAP1 is essential for cell survival and is negatively regulated by HID. *Cell* 98, 453-463.

White, K., Grether, M., Abrams, J. M., Young, L., Farrell, K., and Steller, H. (1994). Genetic Control of Programmed Cell Death in *Drosophila*. *Science* 264, 677-683.

Wilson, R., Goyal, L., Ditzel, M., Zachariou, A., Baker, D. A., Agapite, J., Steller, H., and Meier, P. (2002). The DIAP1 RING finger mediates ubiquitination of Dronc and is indispensable for regulating apoptosis. *Nat Cell Biol* 4, 445-450.

Wing, J. P., Karres, J. S., Ogdahl, J. L., Zhou, L., Schwartz, L. M., and Nambu, J. R. (2002a). *Drosophila* sickle Is a Novel grim-reaper Cell Death Activator. *Curr Biol* 12, 131-135.

Wing, J. P., Schreader, B. A., Yokokura, T., Wang, Y., Andrews, P. S., Huseinovic, N., Dong, C. K., Ogdahl, J. L., Schwartz, L. M., White, K., and Nambu, J. R. (2002b). *Drosophila* Morgue is an F box/ubiquitin conjugase domain protein important for grim-reaper mediated apoptosis. *Nat Cell Biol* 4, 451-456.

Wing, J. P., Schwartz, L. M., and Nambu, J. R. (2001). The RHG motifs of *Drosophila* Reaper and Grim are important for their distinct cell death-inducing abilities. *Mech Dev* 102, 193-203.

Wu, J. W., Cocina, A. E., Chai, J. J., Hay, B. A., and Shi, Y. G. (2001). Structural analysis of a functional DIAP1 fragment bound to grim and hid peptides. *Molecular Cell* 8, 95-104.

Xu, D., Li, Y., Arcaro, M., Lackey, M., and Bergmann, A. (2005). The CARD-carrying caspase Dronc is essential for most, but not all, developmental cell death in *Drosophila*. *Development* 132, 2125-2134.

Yoo, S. J., Huh, J. R., Muro, I., Yu, H., Wang, L., Wang, S. L., Feldman, R. M., Clem, R. J., Muller, H. A., and Hay, B. A. (2002). Hid, Rpr and Grim negatively regulate DIAP1 levels through distinct mechanisms. *Nat Cell Biol* 4, 416-424.

Yu, J., Zhang, L., Hwang, P. M., Kinzler, K. W., and Vogelstein, B. (2001). PUMA induces the rapid apoptosis of colorectal cancer cells. *Molecular Cell* 7, 673-682.

Yuan, J., and Horvitz, H. R. (2004). A first insight into the molecular mechanisms of apoptosis. *Cell* 116, S53-56, 51 p following S59.

Yuan, J., Shaham, S., Ledoux, S., Ellis, H. M., and Horvitz, H. R. (1993). The *C. elegans* cell death gene *ced-3* encodes a protein similar to mammalian Interleukin-1B-converting enzyme. *Cell* 75, 641-652.

Zachariou, A., Tenev, T., Goyal, L., Agapite, J., Steller, H., and Meier, P. (2003). IAP-antagonists exhibit non-redundant modes of action through differential DIAP1 binding. *Embo J* 22, 6642-6652.

Zheng, T. S., Hunot, S., Kuida, K., and Flavell, R. A. (1999). Caspase knockouts: matters of life and death. *Cell Death Differ* 6, 1043-1053.

Zhou, L., Song, Z. W., Tittel, J., and Steller, H. (1999). HAC-1, a *Drosophila* homolog of APAF-1 and CED-4 functions in developmental and radiation-induced apoptosis. *Molecular Cell* 4, 745-755.

Zimmermann, K. C., Ricci, J. E., Droin, N. M., and Green, D. R. (2002). The role of ARK in stress-induced apoptosis in *Drosophila* cells. *J Cell Biol* 156, 1077-1087.

Zong, W. X., Ditsworth, D., Bauer, D. E., Wang, Z. Q., and Thompson, C. B. (2004). Alkylating DNA damage stimulates a regulated form of necrotic cell death. *Genes Dev* 18, 1272-1282.

Zou, H., Henzel, W. J., Liu, X. S., Lutschg, A., and Wang, X. D. (1997). Apaf-1, a human protein homologous to c-elegans ced-4, participates in cytochrome c-dependent activation of caspase-3. *Cell* 90, 405-413.

VITAE

Fatih Akdemir was born in Erzurum, Turkey on January 1st, 1978 to Yahya and Fatma Akdemir. He has an older brother, Gultekin Akdemir. He graduated from Erzurum Science High School in 1995. He received the degree of Bachelor of Science with a major in molecular biology and genetics from Bilkent University in 2000. The same year he moved to Dallas, Texas to attend the Graduate School of Biomedical Sciences at the University of Texas Southwestern Medical Center. In 2001, he married Vildan, and on September 2002 they welcomed a son, Yunus E. Akdemir, into their family.

Permanent Address: 6041 Village Bend Dr, #904
Dallas, TX 75206